

ARM MOVEMENTS DURING SLIPPING

by

Peter Nerses Sandrian III

Bachelor of Science in Mechanical Engineering, Purdue University, 2003

Submitted to the Graduate Faculty of
the School of Engineering in partial fulfillment
of the requirements for the degree of
Master of Science

University of Pittsburgh

2006

UNIVERSITY OF PITTSBURGH

SCHOOL OF ENGINEERING

This thesis was presented

by

Peter Sandrian

It was defended on

August 31, 2006

and approved by

Jean McCrory, Research Assistant Professor, Department of Health and Physical Activity

Mark Redfern, Professor, Department of Bioengineering

Thesis Advisor: Rakié Cham, Assistant Professor, Department of Bioengineering

Copyright © by Peter Sandrian

2006

ARM MOVEMENTS DURING SLIPPING

Peter Sandrian, M.S.

University of Pittsburgh, 2006

Slip-initiated falls often cause injury and death, especially in older adults. Previous research involving perturbed walking has to a large extent focused on lower extremity reactions, yet arm responses are often part of postural reactions to such perturbations. This research is focused on arm responses to an unexpected slip. In Aim 1, the relationship between slip severity and shoulder biomechanics was examined. In Aim 2, we determined if the vestibular system is involved in the triggering of arm responses. The correlation between shoulder moment magnitude and the extent of the body center of mass (COM) perturbation was examined in Aim 3.

Subjects (17 younger and 12 older adults) were exposed to two conditions: (1) baseline dry (subjects knew the floor was dry), and (2) unexpected slip (a diluted glycerol solution was spread on the floor beneath the stance/left foot). Shoulder Euler angles and moments in flexion/extension and abduction/adduction were derived. The spherical elevation angle was used to further describe shoulder kinematics. Slip severity was quantified using measures reported in the literature.

Although arm responses were bilateral, only left (side of slipping foot) shoulder biomechanics, specifically moment generation rates, spherical elevation angle, and abduction angle were positively correlated with slip severity. Left shoulder responses were triggered later than left hip and knee responses. Delayed shoulder moment onsets, slower abduction moment generation rate, and reduced range of motion were found in older adults compared to their younger counterparts. Aim 2 results indicated a weak but statistically significant positive relationship between the timing of the slip-initiated downward head acceleration and the onset of the left shoulder flexion/extension moment (true only when slip severity was controlled in the analysis). In Aim 3, increased left shoulder flexion generation rate correlated with decreased COM perturbation.

In conclusion, evidence presented in this study implies (1) arm responses play a role in balance recovery, (2) a legs-to-arms response sequence appears to drive the reaction to a slip, although the potential implication of the vestibular system cannot be ruled out, (3) age-related effects on arm responses may aggravate the risk of slips and falls in older adults.

TABLE OF CONTENTS

PREFACE	XXI
1.0 SPECIFIC AIMS	1
2.0 INTRODUCTION	3
3.0 ABBREVIATIONS	11
4.0 METHODS	13
4.1 SUBJECTS	13
4.2 EQUIPMENT	14
4.3 CONDITIONS AND PROTOCOL	16
4.3.1 Conditions	16
4.3.2 Protocol	16
4.4 DATA PROCESSING	17
4.4.1 Upper body model and segment definition	17
4.4.2 Shoulder kinematics	20
4.4.3 Shoulder kinetics	22
4.4.3.1 Shoulder moments	22
4.4.3.2 Shoulder joint power	23
4.4.4 Head kinematics	23
4.4.5 COM kinematics	23
4.4.6 Time normalization	24
4.4.7 Parameterization	25
4.4.7.1 Derivation of parameters for Aim 1	25
4.4.7.2 Derivation of parameters for Aim 2	28
4.4.7.3 Derivation of parameters for Aim 3	29
4.5 ANALYSIS	30

4.5.1	Preliminary analysis	30
4.5.2	Specific Aim 1: Shoulder kinetics, kinematics, and Age	31
4.5.3	Specific Aim 1: H3. Timing of shoulders, knees, and hip joints	32
4.5.4	Specific Aim 2. Head acceleration onset and shoulder flexion onset	32
4.5.5	Specific Aim 3. Effect of shoulder moment on COM perturbation	32
5.0	RESULTS	34
5.1	SHOULDER DYNAMICS IN ORDINARY GAIT	34
5.1.1	Shoulder kinematics of ordinary gait.....	34
5.1.2	Shoulder kinetics of ordinary gait.....	39
5.2	SHOULDER DYNAMICS IN RESPONSE TO UNEXPECTED SLIPS.....	43
5.2.1	Shoulder kinematics in slip response: Severity and Age aspects.....	43
5.2.2	Shoulder kinetics in slip response: Severity and Age aspects	54
5.2.3	Comparison of shoulder and leg response timing.....	67
5.3	HEAD ACCELERATION	69
5.3.1	Head COM motion during ordinary gait.....	69
5.3.2	Head COM motion during unexpected slips	70
5.4	EFFECT OF ARM DYNAMICS ON WHOLE BODY COM MOTION	73
6.0	DISCUSSION	77
6.1	SUMMARY OF FINDINGS.....	77
6.2	ARM REACTIONS TO SLIPS	77
6.2.1	Shoulder kinematics and kinetics in slip response.....	77
6.2.2	Age effects in shoulder kinematics and kinetics during slips.....	79
6.2.3	Comparison of shoulder and leg response timing.....	79
6.3	HEAD ACCELERATION	80
6.4	EFFECT OF SHOULDER DYNAMICS ON WHOLE BODY COM MOTION.....	81
7.0	LIMITATIONS	82
8.0	CONCLUSION.....	84
	APPENDIX A	85
	BIBLIOGRAPHY	86

LIST OF TABLES

Table 1. Summary of postural perturbation studies	6
Table 2. Subject profile of age, height, mass, and gender. (As applicable, values are mean \pm standard deviation.).....	13
Table 3. Segment origin and orientation for upper body model segments [27].	18
Table 4. Upper body segment masses, longitudinal COM locations (measured from distal ends of the segments), and radii of gyration [27].	20
Table 5. ANOVA models for Aim 1: H1 and H2	31
Table 6. ANOVA models for Aim 3	33
Table 7. Maximum flexion/extension angles of ensemble average. All units are in degrees.	35
Table 8. Normal gait shoulder angle parameters. Positive values indicate flexion or abduction. Negative values indicate extension or adduction. Statistics shown in boldface indicate significant effects.	38
Table 9. Maximum moments of ensemble average. (All moments are normalized by body mass and have units are N-m/kg.).....	40

Table 10. Normal gait shoulder moment parameters. Positive indicates flexion or abduction. Negative indicates extension or adduction. Moments are normalized by body mass, and have units N-m/kg. Statistics shown in boldface indicate significant effects.	42
Table 11. Quantities of subjects with Onset, and without a conclusive peak value.	44
Table 12. Mean angle change and angle change onset. Onsets times are measured from LHS. All quantities are mean \pm standard deviation.	45
Table 13. ANOVA model of Euler angle Magnitudes, Age, and Hazardousness	50
Table 14. ANOVA model of spherical angle Magnitudes, Age, and Hazardousness	51
Table 15. ANOVA model of Euler angle Magnitudes, Age, and Outcome	51
Table 16. ANOVA model of spherical angle Magnitudes, Age, and Outcome.	51
Table 17. ANOVA model of Euler angle Magnitudes, Age, and PSV.	52
Table 18. ANOVA model of spherical angle Magnitudes, Age, and PSV	52
Table 19. Quantities of subjects with Onset, and without a conclusive peak value.	55
Table 20. Mean shoulder onset times and reactions. All quantities given are mean \pm standard deviation.	56
Table 21. ANOVA model of moment Onset, moment Slope, Age, and Hazardousness. NS indicates no significant effects.	60
Table 22. ANOVA model of moment Onset, moment Slope, Age, and Outcome. NS indicates no significant effects	60

Table 23. ANOVA model of moment Onset, moment Slope, Age, and PSV. NS indicates no significant effects. 61

Table 24. ANOVA model of summed moment Onset, moment Slope, Age, and Hazardousness. 61

Table 25. ANOVA model of summed moment Onset, moment Slope, Age, and Outcome 61

Table 26. ANOVA model of summed moment Onset, moment Slope, Age, and PSV..... 62

Table 27. Summary of statistical results concerning head motion. t_{Az} has a significant effect on t_{LMsum} when controlled for Outcome (* indicates $p < 0.05$). The column ΔR^2 shows the fraction of ANOVA Model 3 that was not explained by model 1; that is, t_{Az} accounts for 16% of the fit in ANOVA Model 3. The head acceleration variable t_{Az} was found to have no significant effect on the movement on the right arm. t_{AZ} had a significant effect on t_{LMsum} (onset of summed left shoulder moment). 72

Table 28. ANOVA models used concerning whole body COM motion and onset of left summed shoulder moment. Only the interaction $Age \times t_{LMsum}$ had significant effects on the difference in θ between BD and SL trials. 76

LIST OF FIGURES

Figure 1. Human Movement and Balance Lab custom marker set. For calibration purposes, all markers are present. In walking trials, including dry and slippery trials, markers beginning with S are not present. Upper body dynamic markers used in this study include head markers (1-4), seventh cervical spine segment (5), inferior end of sternum (6), left and right acromia (7,8), upper arm plate (9-16), forearm plate (17-22), and anterior and posterior superior iliac spine (23-26) markers. Upper body static markers include left and right medial and lateral humeral epicondyles (S1, S2, S3, S4), styloid processes of the left and right radius and ulna (S5, S6, S7, S8), and tenth thoracic segment of the spine (S19) [27]..... 15

Figure 2. Torso, head, upper arm and forearm segment origin and reference frames. The origin of the head local reference frame was located at the top center of the head, and its orthogonal axes are inferior-superior, medial-lateral, and anterior-posterior. The torso local reference frame origin was located at the height of the C7 marker, and had axes pointing inferior-superior, medial-lateral, and anterior posterior. Upper arm local reference frames were located at the elbow joint centers, with the primary axis on the vector from the elbow joint center to the shoulder joint center. Orientation of the remaining axes was determined by the position of the medial and lateral humeral epicondyles. Lower arm reference frame origins were located at their respective wrist joint centers, with the primary axis on the vector from the wrist joint center to the elbow joint center. Orientation of the remaining axes of the lower arm local reference frames was determined by the radial and ulnar styloid processes [27]. Segment origins and orientations are summarized in Table 3..... 18

Figure 3. Definition of alpha angle. α is defined as the included angle between the inferior-superior (Z) axis of the torso local reference frame and the long axis of the upper arm, which lies on the vector from the shoulder joint center to the elbow joint center. Note that pure movement of the elbow in the torso local transverse plane would not affect α . In this diagram, the torso reference frame is depicted at the shoulder for clarity..... 21

Figure 4. Definition of beta angle. β is defined as a projection angle in the transverse (X-Y) plane of the torso local reference frame. The long axis of the upper arm is projected onto this transverse plane. β is the angle between the anterior axis (+X axis in Figure 2) and this projection of the upper arm segment. When the arm is swung rapidly from flexion to extension, or from extension to flexion, β can change very rapidly, even without discontinuities. In this diagram, the torso reference frame is depicted at each shoulder at each shoulder joint center to clarify the angle measure..... 22

Figure 5. The angle θ . θ is measured from a vertical vector through the left heel marker to a vector from the heel through the COM. θ is negative when the COM is behind the heel and becomes positive when the COM is in front of the heel [7]. 24

Figure 6. An example of angle change preceded by passive dynamics. Onset, peak, and magnitude of change resulting from slip are marked. The peak time is chosen as the last data frame within 50% stance, because the SL trend continues monotonically from onset to 50% stance..... 26

Figure 7. Typical trial without deviation. Some parameters in BD and SL trials displayed no evidence of a response to perturbation. Here, the BD and SL trajectories differ as little during slip (post-0%) as they do in the period before slip (-20% to 0%). In this instance, no response is identified for left flexion angle activity. Therefore, no peak is chosen for this parameter..... 26

Figure 8. Typical time history plot of shoulder moment data. For most moment data, a clear onset and peak were visible before 50% stance. Magnitude of the moment data increases rapidly to a peak in the SL trial, and then reverses direction. In that situation, the onset is the point where

the moment data begin to increase in magnitude. Here onset is marked by a vertical line. The peak is the inflection point where the moment data reverses direction, marked here by a short gray line near 36% stance. Slope, determined by the magnitude and duration of the response, is also illustrated. 28

Figure 9. Selection of onset of downward head acceleration. Onset of downward head acceleration was chosen as the post-0% stance peak in head COM vertical acceleration..... 29

Figure 10. Typical example of parameters θ_{40} . θ_{40} is the difference between θ in dry and slip trials at 40% stance. 30

Figure 11. Ensemble averages of left and right shoulder angle. These are averages of one BD trial per subject. Data are time-normalized, with LHS at 0% and LTO at 100%. Shoulder flexion angle is cyclic, with left full extension occurring at or near LHS, and full flexion of the left shoulder occurring shortly after LTO. Flexion/extension range of motion is about 30°. Ab/adduction range of motion is about 8°, or approximately 35% of sagittal plane range. When the right arm is in full extension, the left arm is in full flexion; the reverse is also true. 36

Figure 12. Ensemble averages of spherical angles α and β . (a) An α -value of 180° would indicate that the upper arm were down at the subject’s side, aligned with the torso. An α -value of 0° would indicate that the upper arm were raised to vertical with respect to the torso. Left and right α angle each have local minima at LHS and LTO, meaning that the arms are lifted away from the torso at each heel strike. (b) The left arm is directed backward at heel strike, while the right arm is directed forward. This illustrates the same motion seen in Figure 11a, showing full extension of the left arm at LHS and full flexion of the right arm..... 37

Figure 13. Ensemble averages of left and right shoulder flexion moment in BD trials. At the point when maximum flexion angle is reached, the maximum extension moment is reached. When maximum extension angle is reached, shoulders exert the maximum net flexion moment on the upper arms. The joints generate the greatest torque at maximum flexion and maximum extension because they are changing the direction of arm swing at that time. Abduction moments

are small compared to flexion moments, reaching only half the magnitude of flexion/extension moments. Abduction moment is exerted for the majority of stance. 41

Figure 14. Typical left flexion angle. The left arm in SL trials, which was in extension at heel strike, moved anteriorly in flexion. Thirteen subjects flexed the left arm, and six extended the left upper arm. Ten subjects had no onset. 46

Figure 15. Typical right flexion/extension angle. The vertical line marks the onset of deviation of SL from BD. Seventeen increased the right flexion angle during slip response. Six subjects extended the right arm. Six subjects had no onset. 46

Figure 16. Typical left ab/adduction angle. The vertical line marks the onset of deviation of SL from BD. The upper arm is abducted in response to slip. Twenty-six subjects abducted the left upper arm, and one subject adducted it. Two subjects had no ab/adduction onset. Fifteen subjects continued that response through 50% stance. 47

Figure 17. Typical right abduction angle. The vertical line marks the onset of deviation of SL from BD. The right upper arm is abducted in response to slip. Twenty-five subjects abducted the right shoulder, two adducted, and two had no onset. Seven subjects achieved a local peak in response by 50% stance. 47

Figure 18. Typical left α angle. The vertical line marks the onset of deviation of SL from BD. The α angle combines the upward motion of abduction and flexion: At onset, the gray trend declines quickly as the left arm is raised from the torso, which is due mainly to abduction in this case. Eighteen subjects raised the arms from the torso (as in this figure), four lowered the left arm, and seven subjects had no clear onset. A 180° bias was added to the BD-SL trend. 48

Figure 19. Typical right α angle. The vertical line marks the onset of deviation of SL from BD. The right α angle decreases as the arms are raised from the torso during slip response. Twenty-one subjects had a similar (arm-raising) response, two subjects lowered the arms, and six subjects had no magnitude change in left α angle. A 180° bias was added to the BD-SL trend. . 48

Figure 20. Typical left β angle. The vertical line marks the onset of deviation of SL from BD. The decreasing gray line shows that the subject is moving the arm forward more than left. Fifteen subjects' left β angle decreased (as here), five increased, and nine had no onset. β can change magnitude extremely quickly because of the manner in which it was defined. For instance, if a subject swings the arm from full flexion to full extension in one sweep, passing the elbow next to the torso, β sweeps directly from $\sim 0^\circ$ to $\sim 180^\circ$ 49

Figure 21. Typical right β angle. The long vertical line marks the onset of deviation of SL from BD, and the short vertical line marks the peak. Five subjects increased right β angle as here, thirteen decreased β angle in slip response, and eleven displayed no response. 49

Figure 22. Change of left abduction angle and Hazardousness. ($R^2 = 0.23$) Subjects who experienced hazardous (H) slips also achieved greater changes in left abduction angle. Error bars show standard error..... 52

Figure 23. Change of left flexion angle and Hazardousness. ($R^2 = 0.32$) Older subjects showed either small flexion or small extension angles, while young subjects had flexion angles large. Error bars show standard error..... 53

Figure 24. Change of left abduction angle and Outcome. ($R^2 = 0.18$) Subjects whose Outcomes were classified as Falls (F) achieved greater changes in left abduction angle than those with Outcome Recovery (R). Error bars show standard error. 53

Figure 25. Change of left α angle. ($R^2 = 0.29$) Subjects who fell (F) also tended to raise the arms from the trunk more than those with Outcome Recovery. Error bars show standard error. 54

Figure 26. Change in left abduction angle according to PSV. ($R^2 = 0.27$) Subjects with faster PSV abducted the left shoulder more than subjects with slower PSV ($p_{PSV} < 0.05$). 54

Figure 27. Typical left flexion/extension moment. Left flexion moment normally increased in response to slip, even when kinematics did not reflect this. Onset and peak are illustrated for this case by bars at 31% and 43%, respectively. Seven subjects increased toward flexion moment, twelve subjects increased toward extension moment, and ten had no onset. Of the nineteen subjects with onset, sixteen had peak moment before 50% stance..... 57

Figure 28. Typical right flexion/extension moment. The shoulder exerts a flexion moment (onset marked by long vertical bar), which peaks prior to 50% stance (marked by short vertical bar). Twenty subjects increased flexion moment, and five increased extension moment. Twenty five subjects had discernible onset, and twenty four of those had pre-50% stance peak..... 57

Figure 29. Typical left ab/adduction moment. The long vertical bar indicates onset, and the short vertical bar indicates peak. Twenty five subjects exerted abduction moments and two exerted adduction moments. Twenty seven subjects had onset in response to slip, and twenty five of those subjects had peak moment prior to 50% stance..... 58

Figure 30. Typical right abduction moment. The long vertical bar indicates onset, and the short vertical bar indicates peak. Twenty four subjects increased abduction moment and one exerted an adduction moment. Four other subjects had no distinguishable onset for this variable. 58

Figure 31. Typical left summed moment. The long vertical bar indicates onset, and the short vertical bar indicates peak. Left summed moment is necessarily positive because it is computed from a sum of squares. The summed moment illustrates that subjects develop general increased moment in the shoulder in response to slip events. Twenty-five subjects showed an increased left summed shoulder moment, and none showed a decrease following slip. 59

Figure 32. Typical right summed moment. As for the left summed moment, the right summed moment is always positive and illustrates the tendency to increase net shoulder moment magnitude in response to slips. The long vertical bar indicates onset, and the short vertical bar indicates peak. Twenty-six subjects showed an increase in summed shoulder moment, and no subjects had a decrease in shoulder moment. 59

Figure 33. Onset of left summed moment stratified by Age group and Outcome. ($R^2 = 0.27$) Older adults had later onsets of summed shoulder moments than younger adults. Error bars show standard error. 62

Figure 34. Right abduction moment generation rate stratified by Age group and Outcome. ($R^2 = 0.34$) Older subjects with Outcome Recovery had slower right abduction moment generation rates than older subjects with Outcome Fall. Error bars show standard error. 64

Figure 35. Flexion moment generation rate in the left shoulder compared to PSV. (a) Slope of left should moment generation rate in slip trials ($R^2 = 0.66$, $p_{PSV} < 0.01$). 9 subjects (3 older and 6 younger) had no left flexion moment onset; therefore, the table above has only 20 data points. Subjects with slower PSV tended to also generate increasing flexion moment and those with faster PSV tended to generate increasing extension moments. Age had no significant effect on this relationship ($p_{Age} > 0.10$). (b) Mean left flexion/extension moment generation rate calculated in dry trials, stratified by Hazardousness. Both Hazardous and Non-hazardous groups differed significantly between dry and slip trials (Hazardous slips: $R^2 = 0.83$, $p_{Haz} < 0.01$. Non-hazardous slips: $R^2 = 0.87$, $p_{Haz} < 0.01$). Error bars illustrate standard deviation. 64

Figure 36. Left flexion moment generation rate stratified by Age group and Hazardousness. ($R^2 = 0.85$) Subjects with hazardous (H) slips increased left extensor moments, and those with non-hazardous slips (NH) generated increasing left flexion moments. Older subjects generated moments tending more toward extension, while younger subjects generated moments that tended toward flexion. Error bars show standard error. 65

Figure 37. Left flexion moment generation rate stratified by age group and outcome. ($R^2 = 0.60$) Fallers generated extensor moments in the left shoulder faster than those who recovered. Older subjects with Outcome Recovery generated increasing left flexion moments, while older subjects with Outcome Fall generated increasing extension moments. Younger subjects who recovered tended to generate extension moments significantly slower than older adults experiencing a fall. 65

Figure 38. Left shoulder abduction moment generation rate stratified by age group and Hazardousness. ($R^2 = 0.44$) Subjects with non-hazardous slips generated left abduction moments faster than those who experienced hazardous slips, and older adults generated smaller rates of increase in left abduction moment than younger subjects did. Error bars show standard error. .. 66

Figure 39. Slope of left summed shoulder moment compared to PSV, stratified by Age. ($R^2 = 0.29$) Older subjects who have slow PSV values generated left summed shoulder moments gradually, while older subjects who have fast PSV values generate left summed moment quickly. Younger subjects showed no such trend. 66

Figure 40. Summed left shoulder moment generation rate stratified by age group and outcome. ($R^2 = 0.30$) Subjects who increased their left shoulder moments very quickly tended also to fall. Older subjects with outcome recovery developed summed left shoulder moments significantly slower than older subjects who experienced falls. Such an effect was not evident among younger subjects. Error bars show standard error. 67

Figure 41. Comparison of reactive moment onsets in the left shoulder, knee, and hip, averaged across all subjects. ($R^2 = 0.72$) Subjects initiated left shoulder flexion moment significantly later than both hip flexion moment and knee flexion moment. Error bars show standard error. (* $p < 0.05$) 68

Figure 42. Typical normal HCOM trajectories. Trajectories for one typical subject through the course of an entire BD trial. (Positive = Up/Right/Forward; Negative = Down/Left/Backward) *Vertical* (a, b, c) The head COM moves up and down with the greatest frequency and highest velocity and acceleration. Peaks in the vertical position occur during single-support, and local minima occur at double support. *Mediolateral* (d, e, f) In the M/L direction the head rocks in the direction of the stance foot following each successive heel strike (d, e, f). *Anteroposterior* (g, h, i) In the A/P direction, the head moves steadily forward with relatively constant velocity. In general, maxima or minima of the M/L acceleration curve do not coincide with maxima or minima of the vertical acceleration curve. 70

Figure 43. Comparison of dry/slippy trials. (Positive = Up/Right/Forward; Negative = Down/Left/Backward) In the position graph, only BD-SL is omitted to allow better view of BD and SL trials. PSV in this case is 1.4m/s. *Vertical* (a,b,c) In the acceleration graph, the vertical gray line marks the onset of vertical head acceleration, where the head acceleration in the SL trial peaks after LHS. Little difference was distinguishable between the BD and SL traces before 20% stance in the position graph. The difference is noticeable in the velocity graph only slightly earlier (~15% stance). *Mediolateral* (d,e,f) As the subject slips on the left foot, the head COM moves left, indicated by a decrease in head position. In the velocity and acceleration graphs, no major difference between BD and SL trials occurs until late in the trials. Head velocity in SL trials continues leftward, in contrast to BD trials, where velocity increases to the right. Head acceleration is pointed distinctly to the left as the slip proceeds. *Anteroposterior* (g,h,i) In the position graph, BD and SL plots progress steadily forward together until about 40% stance. In the velocity graph, slight differences in the COM path are highlighted by the first derivative. The acceleration graph shows that as the subject slips, the head COM accelerates backward before returning to almost constant velocity. Deviation of BD and SL A/P acceleration traces was highly variable and often indiscernible because the two traces did not match approaching LHS. 71

Figure 44. Onset of left summed shoulder moment vs. onset of vertical acceleration of the head COM. ($R^2 = 0.29$) Subjects who fell also tend to have later onset of left summed shoulder moment (t_{LMSum}) than those who recovered. Subjects with earlier head acceleration (t_{Az}) tended to have earlier left shoulder moment onset. 72

Figure 45. Ensemble average of θ across dry trials. The trajectory of θ illustrates the path of the COM with respect to the BOS. After heel strike, the COM rises and advances anteriorly with respect the BOS. The dashed lines depict \pm one standard deviation [7]. 73

Figure 46. Typical dry/slippy θ trajectories for one recovery and one fall. The subject who recovers maintains similar trajectories in dry and slippy trials: The COM advances anteriorly and superiorly with respect to the BOS in SL as in BD. In the fall, the subject's θ does not continue to rise much after heel strike, meaning that the BOS remains to the subject's anterior,

and that the COM does not become further elevated. The gray line marks 40% stance, the instant for which θ_{40} is computed [7]. 74

Figure 47. Effect of slope of left flexion moment (S_{LMflex}) on θ_{40} . ($R^2 = 0.58$) There is a negative correlation between θ_{40} and S_{LMflex} ($p_{SLMflex} < 0.01$). Those who exerted extension moments had much lower θ values in the BD trial than in the SL trial, and those with increased flexion moments were likely to have similar θ values in BD and SL trials. Age had no effect on θ_{40} ($p_{Age} > 0.10$). 75

Figure 48. θ_{40} versus onset of left summed moment. ($R^2 = 0.21$) The interaction $Age \times t_{LMsum}$ has a significant effect on θ_{40} , a measure of stability of the COM. Older subjects with early left moment onsets had lower θ_{40} , and older subjects with later left shoulder moment onsets had higher θ_{40} . The opposite was true for younger adults: Those with early left shoulder moment onsets achieved higher θ_{40} , while those with later onsets achieved lower θ_{40} ($p_{Age \times t_{LMsum}} < 0.05$). 76

PREFACE

I would like to thank my thesis advisor, Dr. Rakié Cham, for her effort in this research project. Her vision guided my thesis tremendously. I thank Dr. Mark Redfern and Dr. Jean McCrory for their insight and thoughtful contributions to my study, which they always gave generously and kindly.

Many people contributed to my life and my work in the last two years, in ways subtle and profound that I will not forget. For their unfailing support and encouragement, I thank my friends and my girlfriend Shelly Gabriele. My fellow researchers in the Human Movement and Balance Labs helped me with this project and my coursework: April Chambers answered myriad questions, Leah Enders searched for journal articles, and Dan Steed picked me up from the airport at 11pm. Brooke Coley critiqued parts of this paper and lifted my morale single-handed. Arash Mahboobin was an excellent tutor and faithful critic who gave help each time I asked, and I asked often.

Special thanks to Dr. Brian Moyer for his extraordinary contribution. Brian laid the groundwork for my study by creating the biomechanical model for this study and writing the software to run the model. He also spent many hours - while writing his dissertation - explaining details of the model, and my project depended on him.

My deepest thanks are to Kurt Beschorner. He's been my teacher and constant friend in academics and in life at large. Many hands have guided me in Pittsburgh, and Kurt's has been the steadiest.

1.0 SPECIFIC AIMS

Arms participate in gait and postural response to gait perturbation but their motion remains to be fully quantified and understood. The purpose of this study is to describe arm motions in terms of shoulder kinematics and kinetics during slip events, and quantify differences between older and younger adults, especially in relation to perturbation magnitude. Possible involvement of the vestibular system in the triggering of arm movements in response to unexpected slips will be examined. Finally, the relationship between COM perturbation and shoulder reaction will be explored.

Specific aim 1. Investigate the relationship between slip severity and magnitude/timing characteristics of arm reactions generated in response to unexpected slips

H1. Onset and generation rate of corrective shoulder moments generated in response to slipping depend on slip severity. Magnitude of change of shoulder angle in response to slipping depends on slip severity.

H2. Arm responses to slips will be different in young and older adults. Specifically moment onsets will be delayed in older adults. Also, reduced moment generation rate and response magnitude will characterize arm reactions in older adults compared to young adults. Older adults achieve smaller changes in shoulder angle in response to unexpected slip than younger subjects.

H3. Arm and lower extremity reactions are initiated at approximately the same time.

Specific aim 2. Determine whether the vestibular system is involved in triggering arm responses to unexpected slips.

Hypothesis. Shoulder moment onset in response to unexpected slip is positively correlated with head acceleration onset.

Specific aim 3. Determine whether shoulder moment generation rate impacts whole-body center of mass perturbation.

Hypothesis. Early and faster shoulder moment generation rates will reduce the severity of the COM perturbation.

2.0 INTRODUCTION

Falls are a serious health concern, especially for older and elderly adults. The average annual risk of falling in those aged 65 years and older is at least 30% [6,40,43]. The majority of falls in the general population is attributed to base of support (BOS) perturbations, including slips and trips [6]. Injury resulting from falls worsens with age: In the general population, those aged 85 and older are 7.5 times likelier to be hospitalized due to falls than people aged 65 to 69 years [1]. In fact, 87% of fractures in adults aged 65+ result from falls [36]. Body position, direction, and impact site during falls affect the fall outcome. For instance, forward falls are likelier to cause fractures of the wrist, elbow, and upper arm [30]. Falls to the side are likely to cause injuries to the hips [14].

Falls are a leading cause of injury in the workplace. In the U.S. in 2004, record numbers of fatal and non-fatal workplace injuries from falls were reported [8]. In the years 1989 and 1990, 24% of worker's compensation was paid to fall victims [14]. The total annual cost of falls in those years was about \$50 billion [35]. In Great Britain in 2005, falls precipitated 33% of major workplace injuries, making it the most common cause of major injuries [19]. In Sweden in 1998, falls caused 22% of all occupational accidents [12].

The age of people in the work force is increasing as older people work longer, and because of the increasing age of the workforce, falls in the workplace will probably become more prevalent. Incidence and severity of slip and fall accidents increases with age. In the US in 1992, 18% of all disabling workplace events inflicted on persons age 55 and older were caused by a fall on the same level [32]. In 1995, only 10% of workers in the U.S. were age 55 and older [32]. By 2005, 32% of the work force was age 55 years or older [9]. This age group is expected to continue increasing its share of the labor force through 2008 [18].

Arm activity has been investigated to a lesser extent than lower-limb activity in balance and posture research, as most scientists studying fall-related events address primarily the legs

and trunk, but some researchers recognize the importance of this issue [3,23,29,34,41]. Their studies have shown that direction and use of the arms in dangerous situations is determined by the orientation of the perturbation, and that arm motion affects the progression of slip response [29]. Yet they have not thoroughly characterized arm response to perturbation during steady gait in terms of kinematics, kinetics and onset. There has been no comparison of arm response to factors like slip severity. Some work tests the relationship of muscle activity in arms and legs, and the influence of lower limb proprioception on upper limb response [16], but to our knowledge none test the possibility that the vestibular system spurs arm response.

The role of the arms in gait is not fully understood, especially in response to perturbations. Several theories are offered to explain arm activity during perturbation response. The list includes: (1) Reaching for support, (2) recovering balance by restoring the COM position over a moving base of support, (3) preparing for impact with the ground or other obstacles in the event of a fall, (4) changing momentum to influence the path of the COM, and (5) changing the inertia of the body to slow rotation. These theories are not mutually exclusive. For example, Roberts [37] described a sequence dubbed rescue response, in which perturbed standing subjects invoked (1) Sway reaction - shifting weight in the direction of the perturbation (2) Staggering - moving the feet in the direction of the perturbation force, and, when these fail to recover balance (3) Sweeping reaction, in which the free limbs, including the arms, are used as inertia paddles, so that by imparting momentum on a limb, reaction forces are exerted on the trunk to arrest fall, and eventually, if necessary, (4) Fall-breaking/parachute response, in which the arms are moved to protect the skull from collision. Sweeping response may be a component of righting reflex, mediated by vestibular, visual, and cutaneous senses, by which animals regain upright posture. Current knowledge of the role of arms in ordinary gait, and in perturbed stance and gait, will be reviewed next.

During normal unperturbed steady gait, arm motion is cyclic and in phase with leg motion. It is thought that the angular momentum contribution of the arms reduces the tendency of the body to rotate about the vertical and anterior-posterior axes in single leg stance [17]. The pendular swinging of the arms requires effort from the shoulder and arm muscles, which is present even when the arms are voluntarily constrained, indicating that arm swing is produced from a centrally-determined pattern [4]. At left heel strike (LHS) the left arm is fully extended as the right arm reaches full flexion. As the gait cycle progresses to right heel strike (RHS), the

right arm swings posteriorly to full extension and the left arm swings anteriorly to full flexion. Both arms change direction within 0.1s of each heel strike. Mean sagittal plane rotation of the shoulders is about 25-35°. Sagittal plane shoulder excursion increases during fast gait, and that is due largely to increased extension of the upper arm. Elbow range of motion averages approximately 20° the sagittal plane, and elbow variability is similar to that seen in shoulder motion [28].

Arm motion generated in response to external perturbations has been investigated using different paradigms to disturb balance during standing and gait. The impact of disturbances on arm movements, specifically on arm motion direction, movement magnitude, and onset, has been investigated (Table 1). Arm motion is a prominent, but somewhat non-uniform, part of the response exhibited when balance is perturbed during standing and walking. Several authors reported that in repeated exposures to gait perturbation, all subjects exhibited arm response in each arm, in at least one trial [16,23,25,41]. In repeated perturbations of stance, about 50% of perturbations led to shoulder response [38].

Table 1. Summary of postural perturbation studies

First author	Task: Perturbation	Subject age	Findings
Allum 2003	Stance: Multi-directional platform tilt	Young (20-34) Old (35-55) Elderly(60-75)	Arm response direction depends mainly on direction of trunk in response to perturbation. Young adults and elderly direct trunk movements, and thus arm movements, in opposite directions. Muscle response latencies increase with age. In the presence of a handrail, subjects gazed upon it and grasped it when perturbed. This tendency decreased in repeated trials.
Cejka 2005	Gait: Accelerated walkway	Young (24-35)	Arm and leg muscles have similar response latencies to anterior and posterior accelerations of the foot. Coupling between arm and leg muscles depends on the task being performed at the time of the perturbation.
Dietz 2001	Gait: Fore-aft treadmill	25.5 ± 3.8	Shoulder muscles activated in >85% of trials, and faster perturbations caused greater muscle activation. Shoulder abduction angles increased by 10°-20°. Shoulder and ankle response latencies were similar in response to large-magnitude perturbation. Arm motions are similar for anterior/posterior perturbations, and therefore are not meant to counterbalance. Subjects grasped hand rails in 78% of cases in which they were available.
Maki 1995	Stance: Multi-directional tread mill	23-48	Elevating the arms moves the COM anteriorly after it moves posteriorly with respect to the BOS. Erector spinae and shoulder muscles are activated in slip response. Vertical trajectory change of wrist has latency of ~280ms.
Marigold 2003	Gait: Slip simulated by rollers	21.2 ± 1.2	Rapid arm movements are a common component of perturbation response, and arm movements vary more than leg movements in this response. Response latencies of upper and lower limb muscle activations are similar.
Misiaszek 2003	Gait: Posterior tug at waist	21-28	Subject arm movement slowed forward progression of the COM following slip. Muscle activity in the erector spinae increased in response to slips
Oates 2005	Gait: Rollers at gait termination	24 ± 3	Time required to initiate arm response was the same for active and passive pedaling tasks. Response initiation was faster (40ms) when subjects were not pedaling. Time to grasp a railing was greater in perturbations while pedaling
Quant 2001	Pedaling, still, passive / Seat tilted quickly	19-32	Major shoulder flexion was present in over 50% of trials. Simulations show that arm motions were used most when the COM moved furthest from the BOS. Average shoulder latency was slower than knee, ankle, and torso latency.
Romick-Allen 1988	Stance: Fore-aft tread mill acceleration	Males 20-35	Greater magnitude arm movements, slower muscle onsets, and longer muscle bursts characterized older adult slip response. Back/trunk muscles participated in response.
Tang 1998	Gait: Passive sliding plate	Young (25±4) Older (74±14)	

The role of arm movements generated in response to external perturbations is unclear. In an attempt to fill this research void, studies have investigated whether arm movements are intended to help recover balance independently, or to establish external body support in consideration of environmental surroundings such as hand railings. Direction of arm movements is scrutinized in these studies.

McIlroy and Maki [24] suggested that the arms move to establish support for the body, as by grasping a railing, or to shield the head. They observed arm movements of standing subjects experiencing multi-direction treadmill perturbations at different speeds, with and without a railing present. McIlroy and Maki found that arm movements were directed in the same direction for both forward- and backward-directed platform translations during stance, and inferred that the goal of the movements could not be to counterbalance perturbation [24]. Subsequent work by members of the same research group suggested that grasping movements are controlled differently than responses that occur in environments without hand rails. This response was presumed to rely on the subject's awareness of the presence and location of a putative support [10].

In contrast to the opinion that arm movements are specifically intended to grasp a railing, others surmise that they are intended to counteract the loss of balance, and secondarily take advantage of available supports [25]. Tang and Woollacott note that, despite the presence of hand railings in the experimental setup, none of the older adult subjects grabbed a railing during slip recovery, though it was present during the test [41]. Arm response is not consistently directed toward hand railings when they are present in the experimental setup, which suggests that the primary goal is not to grip a railing. In support of the idea that arms help recover balance, Allum reported that arm movements in young and middle-aged adults were modulated according to perturbation direction [3]. Misiaszek (Table 1) found that it was indistinguishable whether subjects were reaching for railings or attempting to counterbalance their bodies after perturbation. Subjects were inconsistent in their effort to grab the hand rails.

Arm influence on COM path (in slip) brings COM trajectory in the direction of its normal gait path. Oates et al showed with inverse dynamic simulations that without the use of arms, in a situation where subjects slipped while terminating gait, the COM would drop more vertically and deviate more laterally from its usual path [29]. Inverse modeling simulations demonstrated that the contribution of arms in voluntary shoulder flexion (during bipedal stance) kept the whole-

body COM farther forward than it would have been without arms [33]. This is consistent with experimental data: In forward perturbations during stance on a treadmill, the whole-body COM traveled backward farthest when subjects did not exhibit arm-raising response [38]. Large shoulder flexion movements following large trunk hyperextension may stabilize the COM over the base of support provided by the foot or feet [41]. The change in body configuration caused by arm motion could stabilize the body by changing its inertial properties [22].

Onsets of arm movements generated in response to external perturbations are also subject of a debate. Specifically, it is unclear whether arm movements occur at approximately the same time as leg reactions or later than leg reactions, possibly in a sequence of leg-to-upper-body postural responses. For example, in response to treadmill deceleration or waist-jolt perturbations, shoulder muscles fired at about the same time as leg muscles, i.e. 65-95 ms {Dietz et al. 2001} {Misiasek, 2003}. Also, disturbances during gait involving walking on rollers triggered deltoid activity at about 150 ms post-perturbation, at about the same time as tibialis anterior and erector spinae [23]. In contrast, another study found that shoulder muscle activation onsets were considerably later than ankle and knee reactions in response to perturbations of stance [38].

Posture and gait research has not conclusively explained how arm motions are triggered. By electrically stimulating the right tibial nerve at mid-stance, arm and shoulder muscle responses with short latencies were elicited in some subjects {Dietz et al 2001}. Latency of ipsilateral (left) arm and shoulder responses was longer (110-120ms), whereas arm and shoulder latencies of the contralateral side ranged 65-70ms. EMG latencies in response to perturbation are similar in the shoulders and ankles, suggesting that arm movements are not initiated at the end of a legs-to-arms control sequence, but according to Dietz, the vestibular system could play only a very limited role in evoking compensatory reactions in the legs [15]. However, human otolith organs are capable of detecting accelerations as low as 0.063m/s^2 in the anteroposterior direction, 0.057m/s^2 in the mediolateral direction, and 0.154m/s^2 in the vertical direction [5]. Adequate stimulus of semicircular canals to activate vestibulospinal reflex is $0.05^\circ/\text{s}^2$ [15]. Therefore, head motion sensed by the vestibular system may trigger arm response. It has not been proven that the vestibular system, sensitive as it is, has no role in arm compensatory reactions. Indeed, a consistent activation of the gastrocnemius was found to occur 75ms after release of subjects into free-fall, and this response was found to be independent of stretch reflex. Instead, it was

suggested that the mechanism responsible for this muscle activation originated in the otolith organs, caused by acceleration of the head [20].

Responses to perturbed gait change with age. Younger and older adults respond differently to slip events at heel strike and mid-stance [42]. In a study comparing slip reaction strategy of older and younger adults, postural muscle activation in older adults showed increased onset latencies and lesser magnitudes, though the two age groups deployed the same postural muscles. Older adults are likelier to lose balance following slip, to trip with the swing foot, to hyperextend the trunk, and to raise the arms in flexion. Maximum shoulder flexion angle in older adults ranged from about 0~45 degrees, whereas the range in younger adults was about 0°~15° degrees [41]. EMG response magnitude is consistently higher in young subjects than in older or elderly subjects, in gait [41] and in stance [3]. Muscle recruitment is slower in these older and elderly adults.

Response to perturbed stance changes with age, in the same ways that perturbed gait response changes. Allum and colleagues found that, in general, onset latencies increased from young to old, reaction direction changed with age, and magnitude of initial response was weaker with increasing age [3]. This held for ankle, hip, and shoulder/arm muscle responses to the stimulus of an abruptly-tilted floor surface during stance. Onset latencies in elderly were delayed approximately 20-30ms compared to young subjects. Young subjects directed their arm movements opposite the direction of platform tilt, but elderly subjects directed their arm movements in the same direction as the platform tilt, perhaps to break the impending fall. After characteristically brief latencies, younger adults generated strong responses, while elderly subjects generated later responses that were initially weak, but grew in strength as the response progressed for long durations.

The effect of arm motion on gait and slip response is not fully understood. Quantifying the effect of arm motion on the COM would partially explain why the arms are involved in postural response to perturbation.

The literature does not explain the following:

1. Whether arm reaction (moment) onset and magnitude are scaled to the severity of perturbation. How does age affect the reaction of the arms? Previous experiments have shown that large magnitude perturbations of stance spur large-magnitude responses, it follows that arm reaction (moment onset and generation rate) may be scaled to

perturbation severity [24]. Tang and Woollacott point out that in perturbed gait, the magnitude of trunk extension was greatest in older adults, and briefly examine its relationship to maximum shoulder flexion angle [41]. This hints at a relationship between shoulder flexion angle and slip severity, but offers no extensive examination of perturbation magnitude. Such a study is absent in the literature.

2. How arm reactions are triggered. Shoulders muscles respond to perturbations as quickly as leg joints, suggesting that shoulder motion is not initiated as part of a legs-to-arms chain of events. Instead, arm movement may be triggered by pathways whose sensory organs are located in the head: Probably the vestibular rather than the visual system. This study will test for a correlation between head motion onset and shoulder moment onset.
3. How arm motion affects COM trajectory. The consequence of arm motion is not fully understood. Quantifying the effect of arm motion on the COM would partially explain why the arms are involved in postural response to perturbation.

This paper focuses on the activity of arms during slip events, examining the initiation of arm activity, the effect of severity on slips, and age as a factor in precipitating response. It addresses the influence of arms on the body in response to gait perturbation. This will contribute to the understanding of whole-body mechanisms for corrective response to slipping perturbations during gait.

3.0 ABBREVIATIONS

PSV	Peak slip velocity (m/s)
BD	Baseline dry trial
SL	Slip trial
LHS	Left heel strike
RHS	Right heel strike
LTO	Left toe off
RTO	Right toe off
Y	Younger subject age group
O	Older subject age group
R	Recovery: Outcome designation: Pelvis drops by <5% of the minimum height it reached in the BD trial.
F	Fall: Outcome designation: Pelvis drops by >5% of the minimum height it reached in the BD trial.
H	Hazardous Severity designation: PSV > 1.0m/s
NH	Non-hazardous Severity designation: PSV < 1.0m/s
HCOM	Head center of mass
LMflex	Left shoulder flexion moment (N-m/kg)
RMflex	Right shoulder flexion moment (N-m/kg)
LMabd	Left shoulder abduction moment (N-m/kg)
RMabd	Right shoulder abduction moment (N-m/kg)
LMtotal	Left shoulder total moment (N-m/kg)
RMtotal	Right shoulder total moment (N-m/kg)
LAflex	Left shoulder flexion angle (°)
RAflex	Right shoulder flexion angle (°)
LAabd	Left shoulder abduction angle (°)
RAabd	Right shoulder abduction angle (°)
R^2	Square of the regression coefficient
α	In statistical context, the significance level; in this case 0.05.
α	Angular position of the upper arm segment with respect to upward torso axis (°)
β	Projection angle of the upper arm axis onto the torso x-y plane, which is the ~horizontal plane. This angle is defined with respect to the anterior-pointing x-axis (°)

	Onset is the time elapsed between LHS and discerned reaction for SL trials (sec)
t_{Az}	Onset of head acceleration in the Z (sec)
t_{LMflex}	Onset of the Left flexion moment (sec)
t_{RMflex}	Onset of the Right flexion moment (sec)
t_{LMabd}	Onset of the Left abduction moment (sec)
t_{RMabd}	Onset of the Right abduction moment (sec)
t_{LMsum}	Onset of the Left summed moment (sec)
t_{RMsum}	Onset of the Right summed moment (sec)
S_{LMflex}	Rate of change of the Left flexion moment (N-m/kg-s)
S_{RMflex}	Rate of change of the Right flexion moment (N-m/kg-s)
S_{LMabd}	Rate of change of the Left abduction moment (N-m/kg-s)
S_{RMabd}	Rate of change of the Right abduction moment (N-m/kg-s)
$S_{LMtotal}$	Rate of change of the Left total moment (N-m/kg-s)
$S_{RMtotal}$	Rate of change of the Right total moment (N-m/kg-s)
D_{LAflex}	Magnitude of change of the Left flexion angle ($^{\circ}$)
D_{RAflex}	Magnitude of change of the Right flexion angle ($^{\circ}$)
D_{LAabd}	Magnitude of change of the Left abduction angle ($^{\circ}$)
D_{RAabd}	Magnitude of change of the Right abduction angle ($^{\circ}$)
$D_{LA\alpha}$	Magnitude of change of the Left α angle ($^{\circ}$)
$D_{RA\beta}$	Magnitude of change of the Right β angle ($^{\circ}$)
A/P	Anteroposterior
M/L	Mediolateral
Side	Left or right side of the body

4.0 METHODS

The data described in this study were collected as part of a larger slip and fall project. (NIOSH R03-OH007533, Primary investigator R.Cham, PhD.)

4.1 SUBJECTS

Thirty one subjects were recruited for this study in two age groups: Younger (age 20-33) and Older (age 55-67). Participants with a clinically significant history of neurological, orthopedic, cardiovascular and pulmonary abnormalities, and other difficulties preventing normal gait, were excluded based on a phone screening and a neurological screening performed by a clinical neurologist with expertise in balance disorders. Two subjects were excluded from the analysis entirely for watching the floor while walking (1 Old Male subject) and for being a statistical outlier (1 Young Male subject). The remaining 29 subjects' ages and gender are reported in Table 2.

Table 2. Subject profile of age, height, mass, and gender. (As applicable, values are mean \pm standard deviation.)

	Age (years)	Age range (years)	Height (cm)	Mass (kg)	Female	Male
Older subjects	61.1 \pm 3.8	55-67	165.8 \pm 7.7	76.5 \pm 11.8	8	4
Younger subjects	23.9 \pm 3.4	20-33	171.1 \pm 8.4	69.7 \pm 13.2	10	7

4.2 EQUIPMENT

Two Bertec 4060a force plates (Bertec, Columbus, Ohio) embedded in an 8.5m walkway sampled ground reaction forces at 1080Hz. Subjects struck the first force plate with the right foot and the second force plate with the left foot. Ground reaction forces were synchronized with motion data sampled at 120Hz. The floor surface was vinyl tile. An eight M2-camera VICON 612 (VICONPeak, Lake Forest, California) motion measurement system collected 3D motion data at 120Hz. Subjects were marked with 79 passive reflective markers, based on a custom marker set used in the Human Movement and Balance Laboratory (Figure 1).

Movie data were recorded (for qualitative observations only) with a DCR-TRV40 model camcorder (Sony, Oradell, New Jersey). All subjects wore the same model PVC-soled shoes and a uniform spandex (shorts and tank top) outfit. The test setup was illuminated by ceiling mounted halogen lights, which were dimmed during the experiment. To prevent injury, subjects were harnessed to an overhead trolley to prevent hitting the floor in the event of an irrecoverable loss of balance. The trolley was operated by a lab staff member to stay above the subject while walking, and did not impede gait.

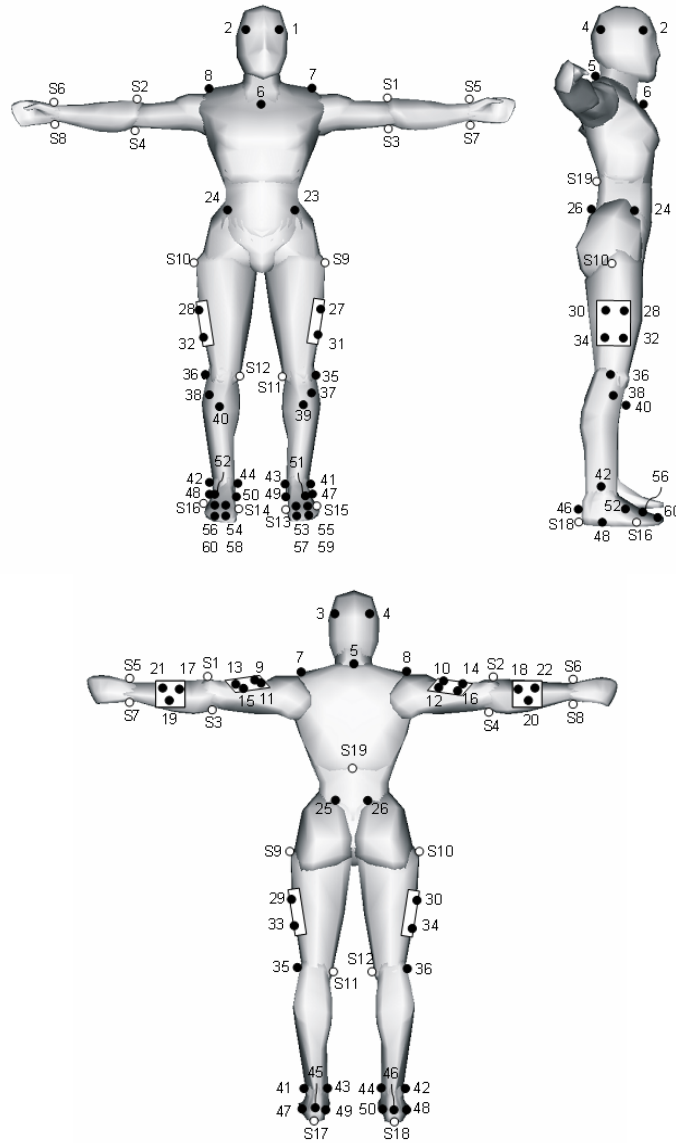


Figure 1. Human Movement and Balance Lab custom marker set. For calibration purposes, all markers are present. In walking trials, including dry and slippery trials, markers beginning with S are not present. Upper body dynamic markers used in this study include head markers (1-4), seventh cervical spine segment (5), inferior end of sternum (6), left and right acromia (7,8), upper arm plate (9-16), forearm plate (17-22), and anterior and posterior superior iliac spine (23-26) markers. Upper body static markers include left and right medial and lateral humeral epicondyles (S1, S2, S3, S4), styloid processes of the left and right radius and ulna (S5, S6, S7, S8), and tenth thoracic segment of the spine (S19) [27].

4.3 CONDITIONS AND PROTOCOL

4.3.1 Conditions

Subjects performed trials under two conditions. Baseline dry (BD) trials are trials in which subjects walk along the dry gait pathway wearing polyvinyl chloride-soled shoes. The coefficient of friction between the dry vinyl floor and shoes was 0.53, as measured with an English XL VIT Slipmeter. Following two or three BD trials, one unexpected slip (SL) trial was collected when, unbeknownst to the subject, a slippery contaminant (75% glycerol, 25% water by volume) was spread on the second (left) force plate. The coefficient of friction of the shoe-floor interface was 0.03 in this condition.

4.3.2 Protocol

After eligibility was confirmed, written informed consent approved by the University of Pittsburgh Institutional Review Board was obtained prior to neurological screening. Anthropometry was recorded. Height, body mass, shoe size, gender, and age were recorded for input to the model. Also, malleolus height, thigh length, calf length, foot length, foot breadth, mid-thigh circumference, calf circumference, knee diameter, malleolus width, and dominant hand were recorded.

All subjects performed the same protocol. Prior to data collection, subjects practiced walking to get accustomed to walking while wearing the marker set and safety harness. During practice, the subject's starting point on the gait path was adjusted so that each foot correctly hit the appropriate force plate. Subjects were instructed to walk as naturally as possible at a self-selected pace. Before each trial, subjects walked to the start of the gait path, faced away from the gait path, and listened to music on head phones for one minute. The music was intended to hide any possible hints about whether the floor would be contaminated. At the end of the minute, subjects were asked to turn around, to focus on an eye-level target at the end of the gait path, and wait for a command to begin walking.

Subjects were told that the first few trials would be non-slippery, to ensure that they walked as naturally as possible. Two or three BD trials were collected, during which researchers

verified that the subject's feet struck the force plates properly. Then, without the subject's knowledge, the contaminant was spread on the left force plate for the slip (SL) trial. The SL trial was carried out so that the subject would not perceive it differently than the previous BD trials.

4.4 DATA PROCESSING

Of the multiple BD trials collected, one trial for each subject was selected for analysis in this study, based on (1) the subject hitting both force plates correctly and (2) successful capture of all markers necessary to complete the model. If several trials met these criteria, the last acceptable dry trial prior to the slip trial was analyzed.

4.4.1 Upper body model and segment definition

The upper body model used to determine Euler angles and joint moments was developed in the Human Movement and Balance Laboratory by Moyer [27] (Figure 2). This custom-written model was defined using BodyBuilder version 3.6 (VICONPeak, Lake Forest, California).

The origin of the torso was located at the height of the C7 marker, with its medial-lateral and anterior-posterior position midway between the C7 and the sternum markers. The reference frame of the torso was constructed by first defining its inferior-superior local axis (Z-axis in Figure 2). Specifically, the orientation of this axis was defined along the vector between the torso origin and the middle of the anterior/posterior superior iliac spines. Next, a temporary vector was defined, pointing from the right acromion to the left acromion. The second axis of the torso local frame (Y-axis in Figure 2) is medial-lateral, pointing to the subject's left, and was taken as the cross product of the Z-vector and this temporary vector. The third axis (X-axis in Figure 2) needed to fully define the torso local reference frame was in the anterior-posterior direction, pointing to the front of the subject, and was derived as the cross product of the inferior-superior and medial-lateral axes.

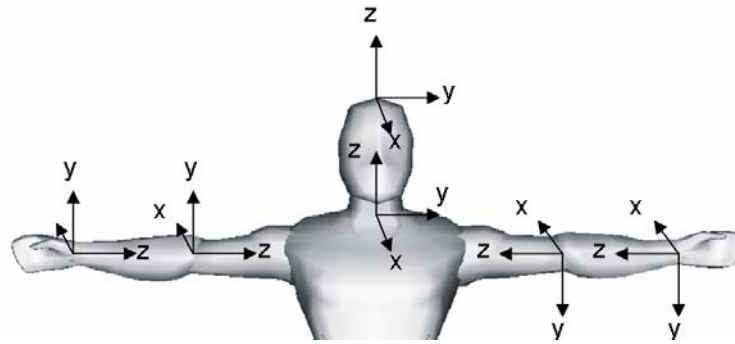


Figure 2. Torso, head, upper arm and forearm segment origin and reference frames. The origin of the head local reference frame was located at the top center of the head, and its orthogonal axes are inferior-superior, medial-lateral, and anterior-posterior. The torso local reference frame origin was located at the height of the C7 marker, and had axes pointing inferior-superior, medial-lateral, and anterior posterior. Upper arm local reference frames were located at the elbow joint centers, with the primary axis on the vector from the elbow joint center to the shoulder joint center. Orientation of the remaining axes was determined by the position of the medial and lateral humeral epicondyles. Lower arm reference frame origins were located at their respective wrist joint centers, with the primary axis on the vector from the wrist joint center to the elbow joint center. Orientation of the remaining axes of the lower arm local reference frames was determined by the radial and ulnar styloid processes [27]. Segment origins and orientations are summarized in Table 3.

Table 3. Segment origin and orientation for upper body model segments [27].

Segment	Origin	First axis	Secondary axis
Torso	Base of the neck	Inferior-superior vector from midpoint of anterior/superior superior iliac spines to	Right acromion to left acromion
Right upper arm	Right elbow joint center	Right elbow joint center to shoulder joint center	Lateral humeral epicondyle to medial humeral epicondyle
Left upper arm	Left elbow joint center	Left elbow joint center to shoulder joint center	Medial humeral epicondyle to lateral humeral epicondyle
Right forearm and hand	Right wrist joint center	Right wrist joint center to elbow joint center	Ulnar styloid process to radial styloid process
Left forearm and hand	Left wrist joint center	Left wrist joint center to elbow joint center	Radial styloid process to ulnar styloid process

The origin of the left upper arm segment was located at the left elbow joint center, ie, midway between the medial and lateral humeral epicondyles. The left upper arm local reference frame was constructed such that the local inferior-superior axis was defined along the vector from the elbow joint center to the shoulder joint center. The shoulder joint center was defined based on the position of the left acromion, according to de Leva [13]. A temporary vector was defined from the lateral humeral epicondyle to the medial humeral epicondyle. The second axis of the left upper arm local reference frame (X vector in Figure 2) is determined by the cross product of this temporary vector and the Z-axis. The third axis (Y-vector in Figure 2) of this reference frame is defined as the cross product of the Z- and X-vectors.

The origin of the right upper arm local coordinate frame was located at the right elbow joint center, and the local inferior-superior axis (Z-axis in Figure 2) lay along the vector between the right elbow joint center and the right shoulder joint center. A temporary vector from the medial to the lateral right humeral epicondyle was defined. The second axis of this reference frame (X-axis of Figure 2) was defined as the cross product of this temporary axis with the local Z-axis. The third axis (Y-axis in Figure 2), pointing roughly in the medial-lateral direction during gait, was defined as the cross product of the local Z- and X-axes.

The origin of the local reference frame of the left forearm and hand segment was located at the left wrist joint center, which was assumed to be at the midpoint of the styloid processes of the radius and ulna. The local inferior-superior axis (Z-axis in Figure 2) lies along the vector from the wrist joint center to the elbow joint center. A temporary vector defined from the radial styloid process to the ulnar styloid process. The second axis (X-axis in Figure 2) was defined as the cross product of this temporary vector with the Z-axis. The third axis (Y-axis in Figure 2) needed to completely define the left forearm local reference frame is the cross product of the Z- and X-axes.

The origin of the local reference frame of the right forearm and hand segment was located at the right wrist joint center, which was assumed to be at the midpoint of the styloid processes of the radius and ulna. The local inferior-superior axis (Z-axis in Figure 2) lies along the vector from the wrist joint center to the elbow joint center. A temporary vector defined from the ulnar styloid process to the radial styloid process. The second axis (X-axis in Figure 2) was defined as the cross product of this temporary vector with the Z-axis. The third axis (Y-axis in

Figure 2) needed to completely define the left forearm local reference frame is the cross product of the Z- and X-axes.

The medial-lateral and anterior-posterior position of the head reference frame origin was in the center of the four head markers, with its vertical position determined by the location of the C7 marker and the measured subject height. The medial-lateral axis (Y-axis in Figure 2) of the head local reference frame contains the anterior head markers. The inferior-superior axis (Z-axis in Figure 2) was perpendicular to the medial-lateral axis and the plane defined by the posterior head markers and C7 marker. The anterior-posterior axis (X-axis in Figure 2) was the cross product of the medial-lateral and inferior-superior axes.

Inertial parameters of all upper body segments were based on the work of de Leva and are summarized in Table 4.

Table 4. Upper body segment masses, longitudinal COM locations (measured from distal ends of the segments), and radii of gyration [27].

Segment	Mass (%)		COM position (%)		R _{ab/adduction}		R _{flex/ext}		R _{int/ext rotation}	
	F	M	F	M	F	M	F	M	F	M
Head	6.68	6.94	48.41	50.02	27.1	30.3	29.5	31.5	26.1	26.1
Torso	30.10	32.29	49.65	50.73	32.8	34.3	29.0	29.4	21.8	23.3
Upper arm	2.55	2.71	42.46	42.28	27.8	28.5	26.0	26.9	14.8	15.8
Forearm and hand	1.94	2.23	32.34	32.49	91.0	102.8	88.1	97.7	9.5	12.3

4.4.2 Shoulder kinematics

Shoulder kinematics were assessed using Euler angles and spherical angles. Euler angles of the shoulders were derived through parent-to-child rotation matrices between each upper arm segment (child) and the torso segment (parent) to find flexion/extension, abduction/adduction, and internal/external rotation angles. For all joints, the order of decomposition was flexion/extension, ab/adduction, and internal/external rotation. These angles were computed in VICON BodyBuilder according to the custom gait model described above [27]. The convention

of the data presented here is that flexion angles are positive while extension angles are negative. Abduction is positive and adduction is negative.

Spherical shoulder joint angles, termed here α and β , are defined according to the globographic method described in [45]. The purpose of examining shoulder activity in this framework was to derive a measure of overall shoulder motion. α is defined as the included angle between the inferior-superior (Z) axis of the torso local reference frame and the long axis of the arm, defined as a vector from the shoulder joint center to the elbow joint center. A person standing in anatomical position would have an alpha angle of approximately 180° , and α decreases as the arm is lifted superiorly. α is constrained between 0° and 180° (Figure 3). Pure movement of the elbow in the torso local transverse plane (X-Y plane in Figure 3) would not affect α .

β is defined as a projection angle in the transverse (X-Y) plane of the torso local reference frame. The long axis of the upper arm is projected onto this transverse plane. β is the angle between the anterior axis (+X axis in Figure 2) and this projection of the upper arm segment. Consequently, β can change very rapidly if the arm is swung in the anterior-posterior direction while close to the torso. However, pure inferior-superior motion of the elbow joint center would not affect β (Figure 4).

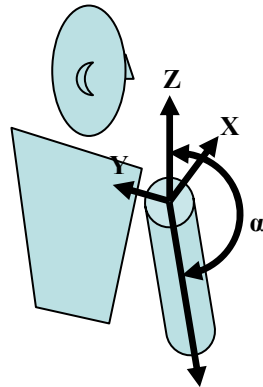


Figure 3. Definition of alpha angle. α is defined as the included angle between the inferior-superior (Z) axis of the torso local reference frame and the long axis of the upper arm, which lies on the vector from the shoulder joint center to the elbow joint center. Note that pure movement of the elbow in the torso local transverse plane would not affect α . In this diagram, the torso reference frame is depicted at the shoulder for clarity.

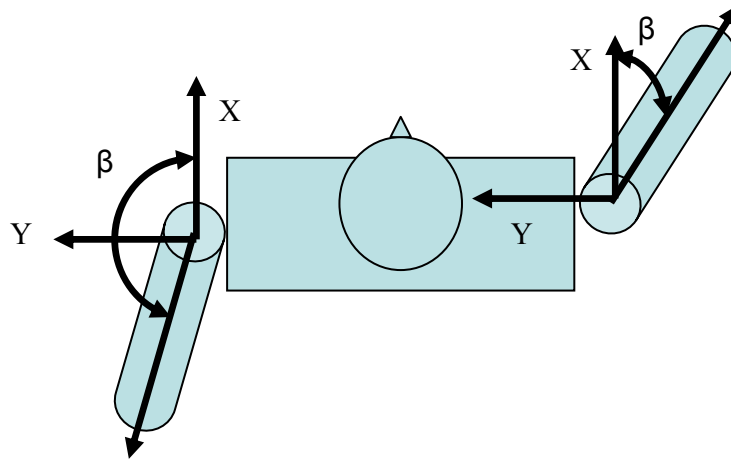


Figure 4. Definition of beta angle. β is defined as a projection angle in the transverse (X-Y) plane of the torso local reference frame. The long axis of the upper arm is projected onto this transverse plane. β is the angle between the anterior axis (+X axis in Figure 2) and this projection of the upper arm segment. When the arm is swung rapidly from flexion to extension, or from extension to flexion, β can change very rapidly, even without discontinuities. In this diagram, the torso reference frame is depicted at each shoulder at each shoulder joint center to clarify the angle measure.

4.4.3 Shoulder kinetics

4.4.3.1 Shoulder moments

Inverse dynamic analysis was used to calculate shoulder joint moments. In the upper body biomechanical model, the joint moments were calculated distal to proximal, that is: Elbow joint moments then shoulder joint moments were computed. The REACTION function in BodyBuilder was used to calculate the forces and moments on the segment's proximal end by accounting for inertial loading, contact loads of the more distal segments, and the external force of gravity. Shoulder joint moments are reported in the reference frame of the torso, and are normalized to body mass. Specifically, flexion-extension moments were calculated about the torso Y-axis and abduction-adduction moments were calculated about the torso X-axis. Two Cartesian components (Ab/adduction and flexion/extension) of the net shoulder moment were also combined for part of this analysis:

$$M_{\text{sum}} = (M_{\text{ab-ad}}^2 + M_{\text{flex-ext}}^2)^{1/2}$$

4.4.3.2 Shoulder joint power

Shoulder joint power in flexion/extension and ab/adduction was derived to provide insight as to whether muscle contributions were concentric or eccentric in generating shoulder torques. Shoulder power was computed using the following formula:

$$P = M * \omega$$

where M = shoulder torque and ω = shoulder angular velocity. The units of power are thus normalized by body mass and have units Watts/kilogram [21,44]. Euler angles were numerically differentiated to calculate angular velocity, in order to calculate joint power. This required that the Euler angle data be filtered. Data were filtered with a zero-phase eighth order low pass elliptic filter (cutoff frequency 6Hz) using Matlab's *filtfilt* command. Numeric derivatives were calculated based on the central difference formula, between adjacent data points, using the Matlab *diff* function, i.e.

$$\dot{x} = \frac{x_{i+1} - x_i}{(1/120s)}$$

4.4.4 Head kinematics

The three-dimensional components of head acceleration in the global reference frame were calculated, a necessary step to achieve Aim 2. First, the head center of mass (HCOM) was found as described above, and its position was reported in the global reference frame. The same elliptic low pass filter described in 4.4.3.2 was used to filter HCOM position data. The second numeric derivative of head position and orientation (angle) was computed using Matlab's *diff* command to find linear acceleration of the head.

4.4.5 COM kinematics

To achieve Aim 3, a measure of the whole-body COM trajectory and perturbation was needed. To account for perturbations both in the direction of travel and in the vertical direction, we used a COM variable developed by Beschorner, et al [7]. First, the entire body was modeled as a linkage of 15 segments, as described by Moyer [27]. To estimate the position of the whole body

COM, a weighted average of segment COM locations was computed [11], based on segment mass distributions of de Leva [13]. The position of this COM was filtered with a zero-phase elliptical filter at 6Hz. The COM position in the sagittal plane is expressed as an angle θ formed by the COM, the left heel marker, and a vertical through the heel marker (Figure 5). θ is negative at heel strike and remains negative until the COM is directly over the ankle, after which θ is positive until the next successive heel strike [7].

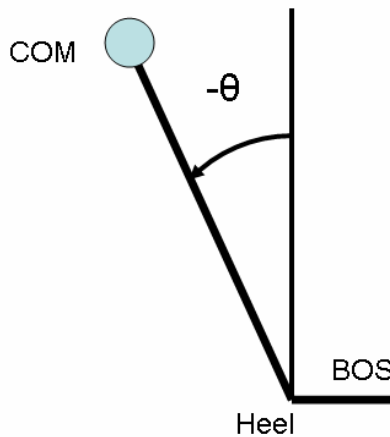


Figure 5. The angle θ . θ is measured from a vertical vector through the left heel marker to a vector from the heel through the COM. θ is negative when the COM is behind the heel and becomes positive when the COM is in front of the heel [7].

4.4.6 Time normalization

The timing of LHS and LTO were determined based on vertical ground reaction forces compared to no-load levels. Heel strike was identified as the first data point at which vertical ground reaction force exceeded the mean plus one standard deviation, as determined from a one-second average unloaded measurement. This point was accepted if the normal force remained larger than one standard deviation and increased to three standard deviations. Heel strike determination was verified by visual inspection of the normal force trace and through inspection of the heel marker vertical displacement. Toe off was determined using the same method, but with the data reversed in time. Data were time normalized with 0% being LHS, and 100% at LTO. Then Matlab's

interp1 command (with option *pchip*, a piecewise cubic Hermite interpolating polynomial) was used to interpolate the data across 2000 points between -50% stance and +150% stance. Each SL trial was time normalized using the time normalization constant of the BD trial that preceded it.

4.4.7 Parameterization

4.4.7.1 Derivation of parameters for Aim 1

The independent kinematic parameters needed to test hypotheses 1 and 2 of Aim 1 consisted of the magnitude of the change in a kinematic variable (D) as a result of slipping. We considered such change for the left/right shoulder angles, both Euler (flexion/extension and ab/adduction) and the spherical angles (α and β). These may be abbreviated D_{LAflex} , D_{RAflex} , D_{LAabd} , D_{RAabd} , $D_{LA\alpha}$, $D_{RA\alpha}$, $D_{LA\beta}$, $D_{RA\beta}$. The change in a kinematic variable as a result of slipping was restricted to the first half of the stance period because beyond 50%, the data in severe slips might have been confounded by two events: (1) the subject might have slipped beyond the contaminated force plate, or (2) the participant might have been caught by the safety harness. As demonstrated in Figure 6, the change in a kinematic variable as a result of slipping was to a large extent determined by

- 1) visually inspecting the time history plot of that variable in the BD trial, in the SL trial, and their difference in normalized time
- 2) manually picking the onset of a deviation (if any) in a kinematic variable from its reference trajectory in the preceding BD trial
- 3) calculating the maximum change in the kinematic variable under consideration from the onset point picked in (2).

Figure 7 demonstrates how sometimes there was no clear deviation in the trajectory of a kinematic variable between SL and BD trials. In that case, the value ‘NaN’ was assigned for the slip-related change in that kinematic parameter, so that it was omitted from analysis.

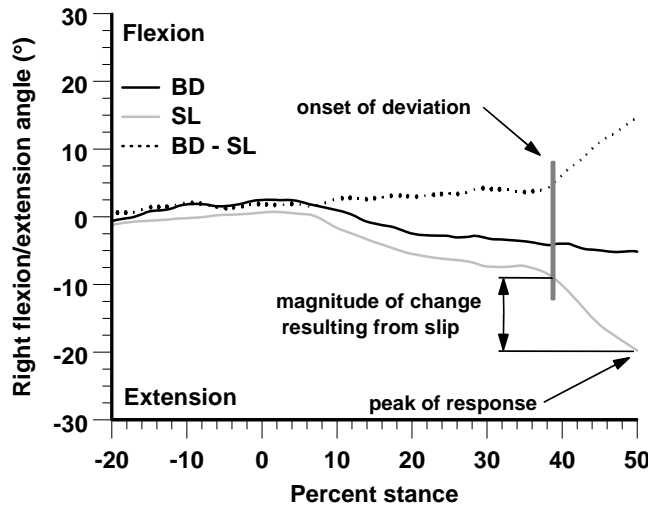


Figure 6. An example of angle change preceded by passive dynamics. Onset, peak, and magnitude of change resulting from slip are marked. The peak time is chosen as the last data frame within 50% stance, because the SL trend continues monotonically from onset to 50% stance.

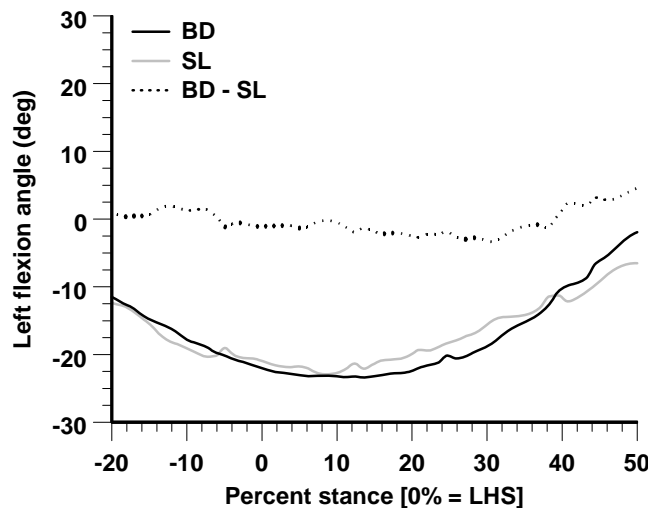


Figure 7. Typical trial without deviation. Some parameters in BD and SL trials displayed no evidence of a response to perturbation. Here, the BD and SL trajectories differ as little during slip (post-0%) as they do in the period before slip (-20% to 0%). In this instance, no response is identified for left flexion angle activity. Therefore, no peak is chosen for this parameter.

The independent kinetic parameters needed to test hypotheses 1, 2, and 3 in Aim 1 consisted of the onset (t) of magnitude change in a kinematic variable as a result of slipping, and

the rate of change (S) of that kinetic variable. We considered such change for the left/right shoulder moments, both Euler (flexion/extension and ab/adduction) and summed moments. Onset may be abbreviated t_{LMflex} , t_{RMflex} , t_{LMabd} , t_{RMabd} , t_{LMsum} , t_{RMsum} , and slope may be abbreviated S_{LMflex} , S_{RMflex} , S_{LMabd} , S_{RMabd} , S_{LMsum} , S_{RMsum} . The change in a kinetic variable as a result of slipping was restricted to the first half of the stance period because beyond 50%, the data in severe slips might have been confounded by two events: (1) the subject might have slipped beyond the contaminated force plate, or (2) the participant might have been caught by the safety harness. As demonstrated in Figure 8, the change in a kinematic variable as a result of slipping was to a large extent determined by

- 1) visually inspecting the time history plot of that variable in the BD trial, in the SL trial, and their difference in normalized time
- 2) manually picking the onset of a deviation (if any) in a kinetic variable from its reference trajectory in the preceding BD trial
- 3) calculating the rate of change in the kinetic variable under consideration from the onset point picked in (2).

As with the kinematic variables, there were cases without clear deviation of the kinetic variable between SL and BD trials. In that case, the value 'NaN' was assigned for the slip-related onset and rate of change in that kinetic parameter, so that it was omitted from analysis.

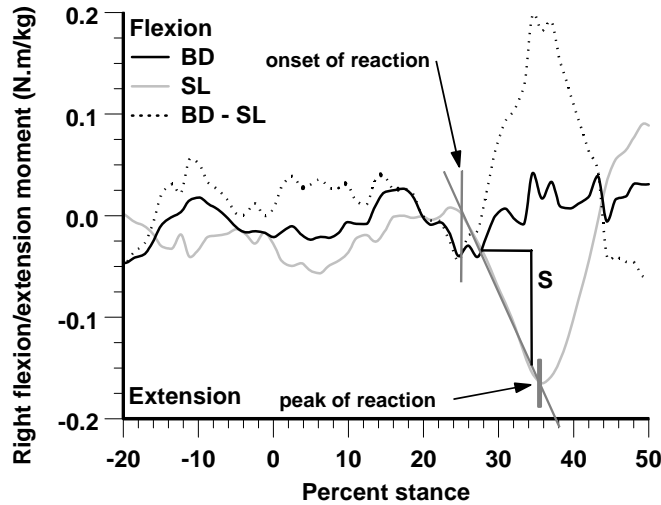


Figure 8. Typical time history plot of shoulder moment data. For most moment data, a clear onset and peak were visible before 50% stance. Magnitude of the moment data increases rapidly to a peak in the SL trial, and then reverses direction. In that situation, the onset is the point where the moment data begin to increase in magnitude. Here onset is marked by a vertical line. The peak is the inflection point where the moment data reverses direction, marked here by a short gray line near 36% stance. Slope, determined by the magnitude and duration of the response, is also illustrated.

Slip severity was quantified using three different measures: Peak slip velocity (PSV), Hazardousness, and Outcome. PSV, a continuous variable, is the local maximum velocity of the heel marker of the slipping (left) foot achieved at least 50ms post-LHS [26]. Hazardousness is determined by PSV. A PSV faster than 1.0m/s was deemed hazardous (H), while those slower than 1.0m/s were deemed non-hazardous (NH). This convention was established in consideration of prior slip research reviewed by Moyer et al [26]. Finally, the Outcome of each SL trial was classified as a Fall or Recovery. A slip was classified as a Fall if the hips dropped below a height 5% lower than the minimum height reached during normal walking. Otherwise, the response was considered a Recovery [31].

4.4.7.2 Derivation of parameters for Aim 2

Onset of acceleration of the head in the vertical direction was examined. The onset of HCOM acceleration in the vertical direction was identified as the instant after LHS when the acceleration curve of the COM of the head in the Z-direction peaked (Figure 9). Shoulder moment onsets and Severity measurements used for Aim 2 were calculated here as they were for Aim 1. Left/right

summed shoulder moment onset was investigated because this was a way of treating the entire joint's response, rather than an individual component of the response.

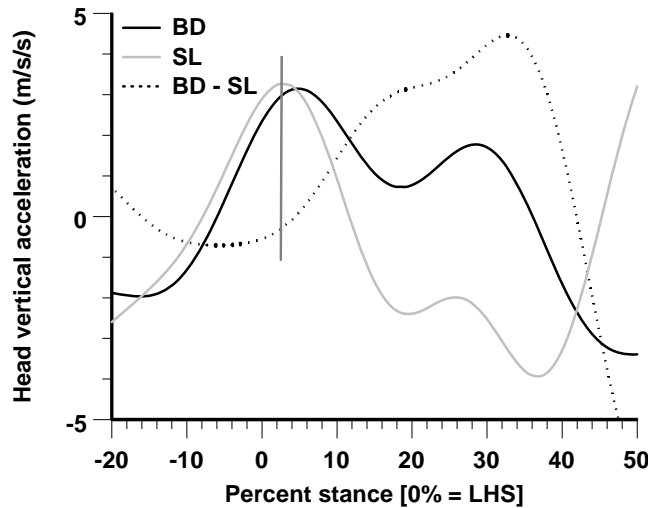


Figure 9. Selection of onset of downward head acceleration. Onset of downward head acceleration was chosen as the post-0% stance peak in head COM vertical acceleration.

4.4.7.3 Derivation of parameters for Aim 3

The difference between θ in BD and SL trials was selected for each subject at 40% stance (θ_{40}). Slopes and onsets of left/right flexion/extension and summed moments, as defined in 4.4.7.1, were also used in this aim.

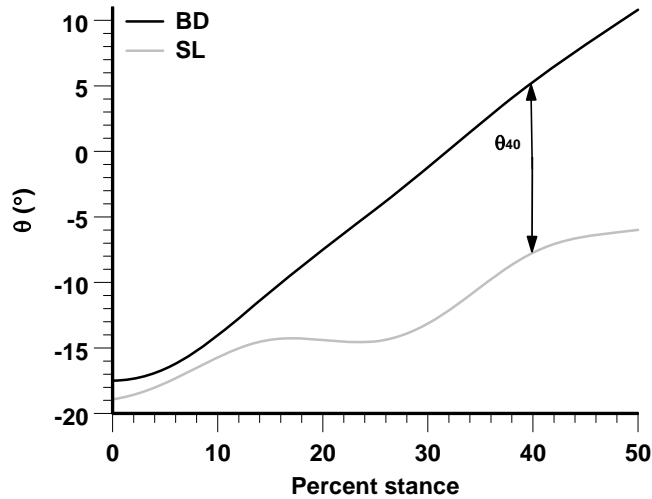


Figure 10. Typical example of parameters θ_{40} . θ_{40} is the difference between θ in dry and slip trials at 40% stance.

4.5 ANALYSIS

For quantitative analysis described, a significance level $\alpha < 0.05$ was used. Normality of each variable was checked with a Shapiro-Wilk test. Non-normal variables were treated with a Box-Cox transformation before applying further analysis.

4.5.1 Preliminary analysis

(Results of this analysis are to be presented in section 5.1)

For visual inspection of shoulder kinetic and kinematic data, time history of the mean and standard deviation of each variable were computed across all subjects. A mixed linear regression model was used to check differences in the main parameters in BD trials, between the left and right sides of the body. Specifically, subject was used as a random effect while body side (left or right), Age, and their interaction were entered as fixed effects. This was done for

- left/right shoulder angles, for flexion/extension, ab/adduction, α , and β
- left/right shoulder moment for flexion/extension, ab/adduction, and summed moments

4.5.2 Specific Aim 1: Shoulder kinetics, kinematics, and Age

(Results of this analysis are to be presented in sections 5.2.1 and 5.2.2.)

H1. Onset and generation rate of corrective shoulder moments generated in response to slipping depend on slip severity.

H2. Arm responses to slips will be different in young and older adults. Specifically moment onsets will be delayed in older adults. Also, reduced moment generation rate and response magnitude will characterize arm reactions in older adults compared to young adults.

Each left/right shoulder kinematic and kinetic parameter was entered individually in a linear regression model including age, slip severity, and their interaction as fixed predictors (Table 5). As mentioned previously, slip severity was assessed using PSV, Hazardousness (Hazardous/Non-Hazardous), or Outcome (Fall/Recovery). A statistical significance level of 0.05 was used. Thus, Hypothesis 1 was proved true if the slip severity factor was significant ($p < 0.05$). Similarly, Hypothesis 2 was proved true if *Age group* was significant ($p < 0.05$). If the factor *Age group x Slip severity* was found statistically significant, further post-hoc Tukey comparison tests were conducted to fully investigate details of this effect.

One additional regression analysis was conducted to determine whether left shoulder flexion/extension moment generation rate differed between dry and slippery trials in subjects who experienced non-hazardous slips: In this mixed linear regression model, “Subject” was entered as a random effect and condition (dry/slippery) was entered as a fixed effect. This analysis was run within Hazardousness groups (H/NH) (Figure 35).

Table 5. ANOVA models for Aim 1: H1 and H2

Dependent variables (one at a time)	Independent variables
Left/right change in shoulder kinematics as a result of slipping	Age
Onset of left/right change in shoulder moments as a result of slipping	Slip severity*
Slope of left and right shoulder moments as a result of slipping	Age x Slip severity*

* Slip severity = PSV, Hazardousness (Hazardous/Non-Hazardous), or Outcome (Fall/Recover)

4.5.3 Specific Aim 1: H3. Timing of shoulders, knees, and hip joints

(Results of this analysis are to be presented in 5.2.3.)

H3. Arm and lower extremity reactions are initiated at approximately the same time.

A mixed linear model - with subject as a random effect, and joint (shoulder, knee, hip) moment onset as a fixed effect – was used to compare reaction times of hip, knee, and shoulders on the left side of the body. Hypothesis 3 was proved true if onsets of knee, hip, and shoulder moment onsets were not significantly different, as shown by, i.e. $p < 0.05$. If $p < 0.05$, post-hoc Tukey comparison tests were conducted to fully investigate details of this effect.

4.5.4 Specific Aim 2. Head acceleration onset and shoulder flexion onset

(Results of this analysis are to be presented in 5. 3.)

Hypothesis: Shoulder moment onset in response to unexpected slip is positively correlated with head acceleration onset.

Shoulder moment onset was entered as the dependent variable in a regression model including vertical head acceleration onset as the predictor. Also, Outcome was used as a covariate to control slip severity effects.

4.5.5 Specific Aim 3. Effect of shoulder moment on COM perturbation

(Results of this analysis are to be presented in 5.4.)

Hypothesis: Early and faster shoulder moment generation rates will reduce the severity of the COM perturbation.

Linear regression models were used to test the dependence of the whole-body COM perturbation on the onset or generation rate of shoulder moments. Specifically, θ_{40} was the dependent variable, and one kinetic parameter, Age, and their interaction, were set as fixed effects (Table

6). θ_{40} was compared with left/right flexion/extension moment generation rates and summed shoulder moment generation rates, and their onsets, to test whether the summed shoulder moment generation rate affected the perturbation of the COM. θ_{40} was compared with flexion/extension moment generation rates, and the associated onsets, because these slope parameters account for directional differences in flexion (positive) and extension (negative) moments.

Table 6. ANOVA models for Aim 3

Dependent variable	Independent variables
θ evaluated at 40% stance	Age Kinetic variable* Age x Kinetic variable*

* Kinetic variable = Left/right onset of moment, or moment generation rate in flexion/extension and summed moment

5.0 RESULTS

5.1 SHOULDER DYNAMICS IN ORDINARY GAIT

5.1.1 Shoulder kinematics of ordinary gait

Flexion/extension angles Ensemble averages of left and right shoulder angle show that flexion/extension angles are cyclic. Left full extension (13.5°) occurs at or near LHS, and full flexion of the left shoulder (16.3°) occurs shortly after LTO. Ranges of left and right average flexion/extension motion are about 30° and 23° , respectively (Table 7). When the right arm is in full extension, the left arm is in full flexion; the reverse is also true (Figure 11a). Younger subjects had lower maximum right flexion angle than left flexion angle. This distinction was not present in older adults ($p_{\text{AgeXSide}} < 0.01$, Table 8).

Abduction/adduction angle Ab/adduction range of motion is about 5° , or approximately 17% of sagittal plane range (Table 7). The arm is gradually abducted as it swings forward into flexion (Figure 11b). The mean right abduction angle is greater than the mean left abduction angle ($p_{\text{Side}} < 0.05$), and the maximum right abduction angle attained was greater than that attained in the left arm ($p_{\text{Side}} < 0.05$). Older subjects had greater abduction angles than younger subjects (mean: $p_{\text{Age}} < 0.01$).

Table 7. Maximum flexion/extension angles of ensemble average. All units are in degrees.

Angle	Left shoulder (°)	Right shoulder (°)
Mean maximum flexion	13.5 ± 9.8	9.3 ± 9.9
Mean maximum extension	16.3 ± 6.4	13.6 ± 10.7
Flexion/extension range	29.7	22.9
Mean maximum abduction	11.6 ± 5.8	12.6 ± 5.9
Mean maximum adduction	6.6 ± 6.0	8.1 ± 5.3
Ab/adduction range	5.0	4.5

Spherical angles α and β An α -value of 180° would indicate that the upper arm were down at the subject's side, aligned with the torso. An α -value of 0° would indicate that the upper arm were raised to vertical with respect to the torso. Left and right α angle each have local minima at LHS and LTO, meaning that the arms are far from the torso at each heel strike (Figure 12a). The β angle shows that the left arm is directed backward at heel strike, while the right arm is directed forward. This illustrates the same motion seen in Figure 11a, showing full extension of the left arm at LHS and full flexion of the right arm. Older subjects have a smaller spherical α -angle (i.e., carry the upper arms higher) than young subjects ($p_{\text{Age}} < 0.01$, Table 8), confirming the finding that older subjects have higher ab/adduction angles. Also, younger subjects maintained a greater average α in the right and left arms than older adults maintained in the right arm (Table 8 - mean: $p_{\text{Age} \times \text{Side}} < 0.05$). Young subjects maintained greater minimum α -angle in the right arm than older subjects maintained in the left arm (Table 8 - minimum: $p_{\text{Age} \times \text{Side}} < 0.01$).

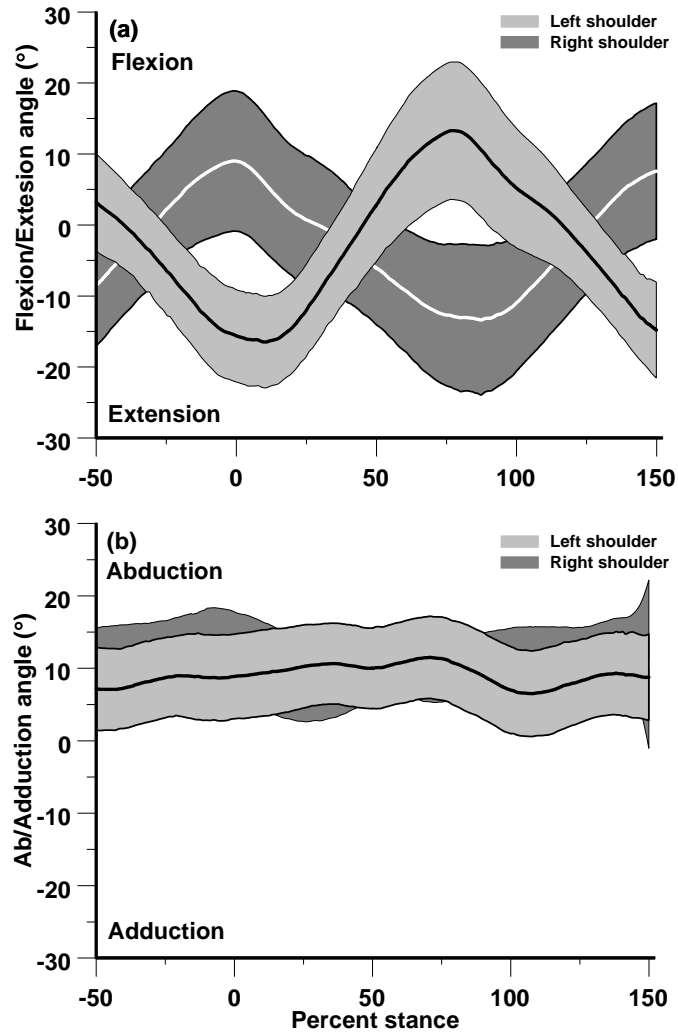


Figure 11. Ensemble averages of left and right shoulder angle. These are averages of one BD trial per subject. Data are time-normalized, with LHS at 0% and LTO at 100%. Shoulder flexion angle is cyclic, with left full extension occurring at or near LHS, and full flexion of the left shoulder occurring shortly after LTO. Flexion/extension range of motion is about 30°. Ab/adduction range of motion is about 8°, or approximately 35% of sagittal plane range. When the right arm is in full extension, the left arm is in full flexion; the reverse is also true.

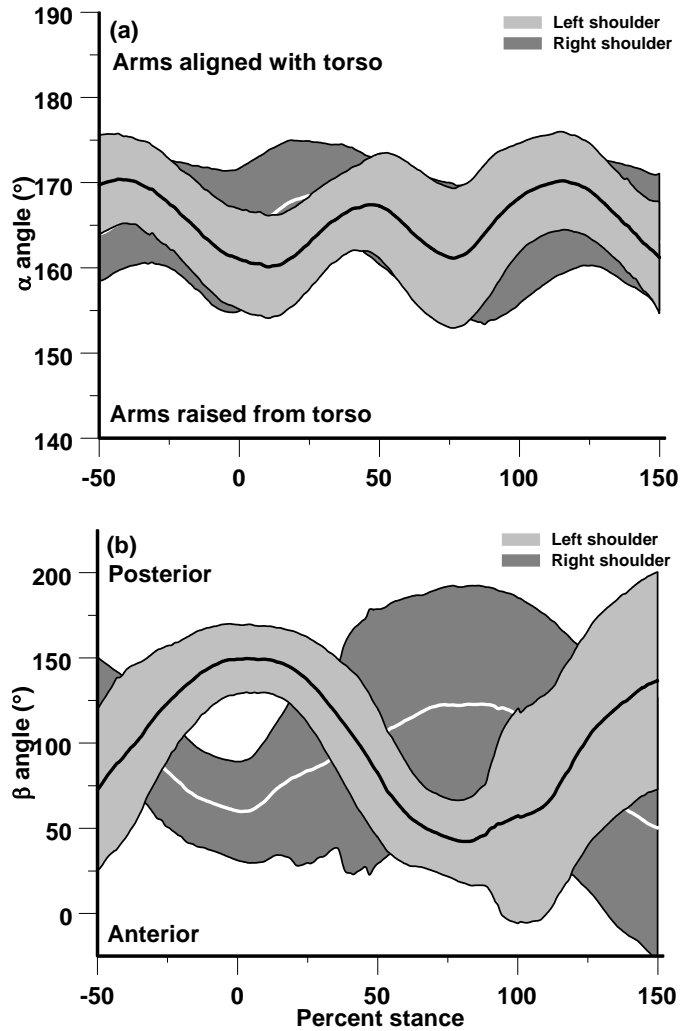


Figure 12. Ensemble averages of spherical angles α and β . (a) An α -value of 180° would indicate that the upper arm were down at the subject's side, aligned with the torso. An α -value of 0° would indicate that the upper arm were raised to vertical with respect to the torso. Left and right α angle each have local minima at LHS and LTO, meaning that the arms are lifted away from the torso at each heel strike. (b) The left arm is directed backward at heel strike, while the right arm is directed forward. This illustrates the same motion seen in Figure 11a, showing full extension of the left arm at LHS and full flexion of the right arm.

Table 8. Normal gait shoulder angle parameters. Positive values indicate flexion or abduction. Negative values indicate extension or adduction. Statistics shown in boldface indicate significant effects.

		Old		Young		Statistics
		Left	Right	Left	Right	p-value
Flexion/extension angle	Mean	-5.1 ± 5.2°	-1.7 ± 11.1°	-1.4 ± 6.2°	-3.23 ± 5.1°	p _{Side} > 0.10 p _{Age} > 0.10 p _{Age X Side} ≤ 0.10
	Maximum	9.68 ± 7.9°	11.4 ± 11.2°	16.5 ± 8.5°	8.3 ± 7.2°	p _{Side} ≤ 0.10 p _{Age} > 0.10 p_{Age X Side} < 0.01
	Minimum	-17.9 ± 4.9°	-15.8 ± 12.7°	-17.5 ± 7.2°	-14.4 ± 8.7°	p _{Side} > 0.10 p _{Age} > 0.10 p _{Age X Side} > 0.10
Abduction/adduction angle	Mean	11.7 ± 5.1°	14.3 ± 4.2°	6.8 ± 4.6°	8.5 ± 3.4°	p_{Side} < 0.05 p_{Age} < 0.01 p _{Age X Side} > 0.10
	Maximum	15.6 ± 4.9°	18.0 ± 4.7°	10.9 ± 4.3°	12.44 ± 5.0°	p_{Side} < 0.05 p_{Age} < 0.01 p _{Age X Side} > 0.10
	Minimum	8.2 ± 5.6°	10.4 ± 4.6°	2.8 ± 5.0°	1.2 ± 12.5°	p _{Side} > 0.10 p_{Age} < 0.01 p _{Age X Side} > 0.10
α angle	Mean	164.1 ± 4.6°	160.9 ± 5.9°	166.7 ± 4.3°	167.6 ± 4.6°	p _{Side} > 0.10 p_{Age} < 0.01 p_{Age X Side} < 0.05
	Maximum	170.3 ± 5.7°	166.3 ± 5.1°	175.1 ± 4.2°	173.4 ± 3.6°	p_{Side} < 0.01 p_{Age} < 0.01 p _{Age X Side} > 0.10
	Minimum	156.9 ± 4.3°	153.8 ± 7.5°	156.1 ± 7.5°	161.1 ± 8.3°	p _{Side} > 0.10 p _{Age} > 0.10 p_{Age X Side} < 0.01

Table 8 (continued).

β angle	Mean	108.2 ± 18.4°	96.6 ± 29.8°	94.1 ± 28.8°	90.2 ± 60.8°	p _{Side} > 0.10 p _{Age} > 0.10 p _{Age X Side} > 0.10
	Maximum	149.1 ± 15.2°	133.9 ± 32.7°	158.9 ± 21.3°	147.3 ± 24.6°	p _{Side} < 0.05 p _{Age} > 0.10 p _{Age X Side} > 0.10
	Minimum	54.9 ± 27.9°	60.2 ± 23.0°	-14.0 ± 81.7°	14.3 ± 81.7°	p _{Side} > 0.10 p_{Age} < 0.01 p _{Age X Side} > 0.10

5.1.2 Shoulder kinetics of ordinary gait

Flexion/extension moment Shoulder flexion/extension moment is cyclic, and out of phase with shoulder flexion angle. At the point when maximum flexion angle is reached, the maximum extension moment (0.065N-m/kg) is reached. When maximum extension angle is reached, shoulders exert the maximum net flexion moment (0.057N-m/kg) on the upper arms. (Maximum and minimum values of the ensemble averages are shown in

Table 9). The joints generate the greatest torque at maximum flexion and maximum extension because they are changing the direction of arm swing at that time (Figure 13a). Left flexion moments were greater than right flexion moments (Table 10 - mean: p_{Side} < 0.01).

Abduction moment Abduction moments are small compared to flexion moments, reaching only half the magnitude of flexion/extension moments. Abduction moment is prevalent compared to adduction moment. While the arm is moving posteriorly (into extension), an abduction moment (approximately 0.036N-m/kg) is being exerted. As the arm moves posteriorly and the shoulder is flexed, the shoulder moment tends toward relaxation or adduction (approximately 0N-m/kg) (Figure 13b). Older subjects had greater abductor moments than

younger subjects (Table 10 - mean: $p_{\text{Age}} < 0.05$), and maximum abduction moments reached were greater in the left shoulder than in the right (Table 10 - max: $p_{\text{Side}} < 0.05$).

Table 9. Maximum moments of ensemble average. (All moments are normalized by body mass and have units are N-m/kg.)

Moments	Left shoulder	Right shoulder
Maximum flexion	0.065 ± 0.035	0.050 ± 0.029
Maximum extension	0.057 ± 0.028	0.041 ± 0.034
Flexion/extension range	0.122	0.091
Maximum abduction	0.036 ± 0.019	0.030 ± 0.020
Maximum adduction	-0.002 ± 0.014	0.002 ± 0.013
Ab/adduction range	0.038	0.028

Summed moment The summed moment is positive at all times because it is computed from the squares of flexion/extension and ab/adduction moments, and clearly reflects the local maxima and minima of the flexion/extension moment. The contribution of the ab/adduction moment is of lower magnitude, and thus less prominent in summed moment (Figure 13c). The summed moment generated in the left shoulder was greater than that in the right shoulder, which agrees with the flexion and abduction moment data (mean: $p_{\text{Side}} < 0.01$). Young subjects maintained lesser average summed moments in the right shoulder than in the left shoulder, and young subjects maintained lesser average summed moments in the right shoulder than older subjects maintained in either shoulder (Table 10 - $p_{\text{Age} \times \text{Side}} < 0.01$). In general, older subjects' shoulders exerted greater moments than younger subjects' shoulders (Table 10 - min: $p_{\text{Age}} < 0.01$).

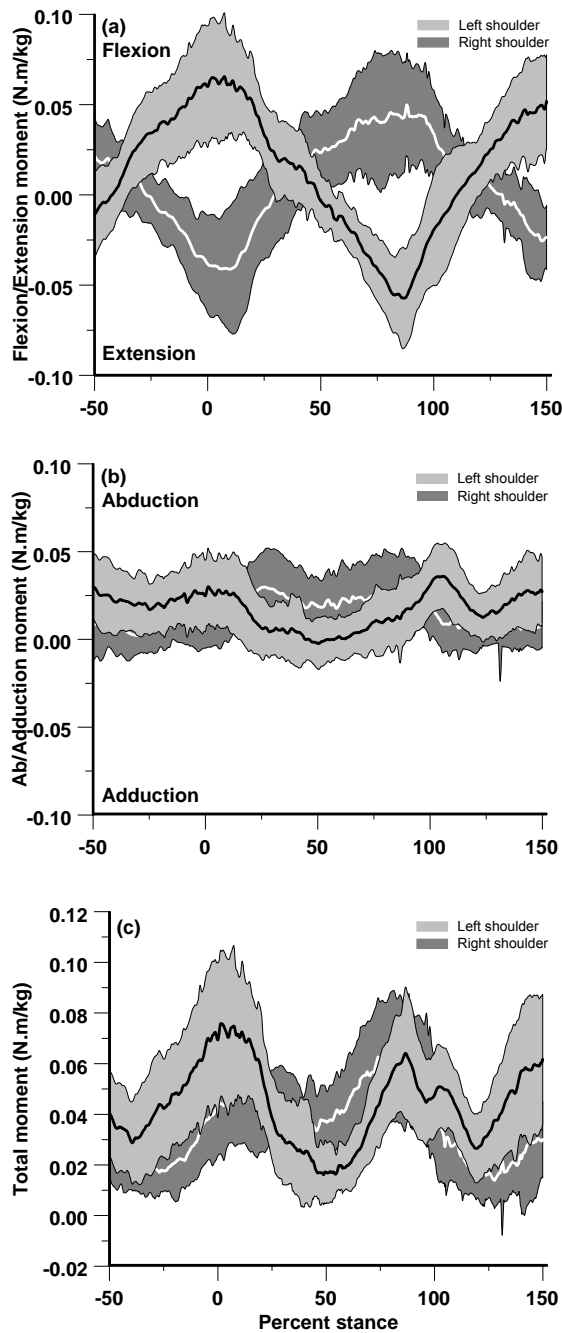


Figure 13. Ensemble averages of left and right shoulder flexion moment in BD trials. At the point when maximum flexion angle is reached, the maximum extension moment is reached. When maximum extension angle is reached, shoulders exert the maximum net flexion moment on the upper arms. The joints generate the greatest torque at maximum flexion and maximum extension because they are changing the direction of arm swing at that time. Abduction moments are small compared to flexion moments, reaching only half the magnitude of flexion/extension moments. Abduction moment is exerted for the majority of stance.

Table 10. Normal gait shoulder moment parameters. Positive indicates flexion or abduction. Negative indicates extension or adduction. Moments are normalized by body mass, and have units N-m/kg. Statistics shown in boldface indicate significant effects.

		Old		Young		Stats
		Left	Right	Left	Right	p-value
Flexion/extension moment	Mean	0.0120 ± 0.0092	0.0032 ± 0.0101	0.0155 ± 0.0088	0.0076 ± 0.0087	p_{Side} < 0.01 p _{Age} > 0.10 p _{AgeXSide} > 0.10
	Maximum	0.0840 ± 0.0298	0.0758 ± 0.0372	0.0934 ± 0.0277	0.0694 ± 0.0253	p_{Side} < 0.05 p _{Age} > 0.10 p _{AgeXSide} > 0.10
	Minimum	-0.0639 ± 0.0299	-0.0654 ±0.0358	-0.0673 ±0.0223	-0.0584 ± 0.0278	p _{Side} > 0.10 p _{Age} > 0.10 p _{AgeXSide} > 0.10
Abduction/adduction moment	Mean	0.0230 ±0.0358	0.0174 ±0.0074	0.0121 ±0.0087	0.0130 ±0.0056	p _{Side} > 0.10 p_{Age} < 0.05 p _{AgeXSide} > 0.10
	Maximum	0.0636 ± 0.0134	0.0531 ± 0.0209	0.0562 ± 0.02021	0.0475 ± 0.0125	p_{Side} < 0.01 p _{Age} > 0.10 p _{AgeXSide} > 0.10
	Minimum	-0.0193 ± 0.0228	-0.0152 ± 0.0249	-0.0246 ± 0.0121	-0.0269 ± 0.0305	p _{Side} > 0.10 p _{Age} > 0.10 p _{AgeXSide} > 0.10
Summed moment	Mean	0.0423 ± 0.0117	0.0425 ± 0.0107	0.0438 ± 0.0069	0.0323 ± 0.0069	p_{Side} < 0.01 p _{Age} > 0.10 p_{AgeXSide} < 0.01
	Maximum	0.0979 ±0.0295	0.0945 ±0.0277	0.1033 ±0.0241	0.0851 ±0.0311	p _{Side} > 0.10 p _{Age} > 0.10 p _{AgeXSide} > 0.10
	Minimum	0.0046 ±0.0048	0.0062 ±0.0044	0.0021 ±0.0018	0.0023 ±0.0026	p _{Side} > 0.10 p_{Age} < 0.01 p _{AgeXSide} > 0.10

5.2 SHOULDER DYNAMICS IN RESPONSE TO UNEXPECTED SLIPS

5.2.1 Shoulder kinematics in slip response: Severity and Age aspects

Typical trials of flexion/extension (Figure 14 and Figure 15), ab/adduction (Figure 16 and Figure 17), and spherical angles α and β (Figure 17, Figure 18, Figure 19 and Figure 20) show the angular position pattern followed by most subjects' trajectories. Typical patterns presented below illustrate patterns in the data exhibited by many of the subjects. This is meant to give a general idea of tendencies in the data, however, in many cases, no onset occurred between 0% and 50% stance. Also, several subjects who displayed onset in response to slip did not complete their entire response by the 50%-mark, the point beyond which data were not considered. Left/right ab/adduction angles appeared more consistently than flexion/extension and β angles (Table 11). The shoulder trajectories in BD and SL trials of a given subject were usually very close until about 30% stance. If onset occurred for a trajectory or moment in SL, it was generally preceded by a slight change from BD, which might begin around 15% or 30% stance. Then a sharper change occurred, marking the onset (Figure 16).

The mean response times/magnitudes of old/young subjects are shown in Table 12. In 66% of SL trials a flexion/extension response was seen in the left arm, which was at full extension at heel strike during normal walking. In 68% of those positive responses, the left upper arm moved anteriorly in flexion, and the other 32% of subjects displayed an extension response. Ten subjects (34%) had no left flexion/extension onset (Figure 14). 79% of subjects had discernible flexion/extension response in the right arm, and 74% of those resulted in flexion, while the remaining 26% resulted in extension. 26% of subjects had no distinct flexion/extension response in the left arm (Figure 15).

Abduction/adduction responses were clearer than flexion/extension responses. 93% of subjects had left ab/adduction response, 96% of those being abduction movements, and 4% adduction motions (Figure 16). 93% of subjects showed very different right ab/adduction kinematics in BD and SL trials, and 56% of them continued the response through 50% stance. 93% of those were abduction responses; the remaining 7% were adduction responses (Figure 17).

Table 11. Quantities of subjects with Onset, and without a conclusive peak value.

Parameter	Have onset pre-50%	Subjects with peak at 50%	PSV(m/s) of subjects without onset
Left flexion angle	19	12	O 1.2, 1.1, 2.2, 0.8 Y 2.1, 1.2, 1.3, 0.5, 0.5, 0.6
Right flexion angle	23	15	O 0.8, 0.8, 0.8 Y 2.1, 1.2, 0.5
Left abduction angle	27	20	O 0.8 Y 0.5
Right abduction angle	26	6	O 1.1 Y 0.5, 0.6
Left α angle	20	19	O 1.1, 2.2, 1.9 Y 0.5, 1.1, 0.5, 0.6
Right α angle	24	18	O 1.1, 0.8 Y 0.5, 2.1, 0.6
Left β angle	20	16	O 1.2, 1.1, 1.8, 0.8 Y 2.1, 1.3, 0.6, 1.5, 1.9
Right β angle	18	12	O 1.1, 1.3, 0.8 Y 2.1, 1.2, 1.5, 1.3, 0.5, 0.5, 0.6, 0.6

The interpretation of shoulder motions as spherical angles is most consistent in terms of α angle, which combines the superiorly-oriented motion of abduction and flexion, and the inferiorly-oriented motion of flexion and adduction. Only 76% of subjects displayed a great difference between BD and SL trials in left shoulder α angle (Figure 18). 82% of subjects with left arm response decreased α angle of the left shoulder (moved the arm superiorly), and 18% increased α angle (moved the arm inferiorly). 79% of subjects showed α angle response in the right arm, and 91% of them elevated the right arm, while the remaining 9% lowered the right arm (Figure 19).

β angle shows mainly the anterior-posterior position, which is primarily determined by flexion/extension angle in large arm movement, and β angle motion was less frequently

identified than other angles examined here. Only 69% had a left shoulder β angle response, and 75% of those were decreases, indicating anterior movement of the upper arm (Figure 20). The remaining 25% of left β angle movements were increases, showing posterior movement of the arm. 62% of subjects had distinguishable right arm β angle responses, of which 72% were decreases and 28% were increases (Figure 21 and Figure 20).

Table 12. Mean angle change and angle change onset. Onsets times are measured from LHS. All quantities are mean \pm standard deviation.

		Flex/extension		Ab/adduction		α -angle		β -angle	
		Onset (ms / %)	Change ($^{\circ}$)						
Left	O	256 \pm 52	3.2	240 \pm 39	7.0	257 \pm 33	-4.9	262 \pm 50	-15.3
		38.7 \pm 6.3	\pm 7.7	36.7 \pm 6.1	\pm 5.2	38.6 \pm 4.1	\pm 7.1	39.3 \pm 6.5	\pm 20.3
Left	Y	244 \pm 39	12.3	237 \pm 44	8.4	251 \pm 46	-8.3	267 \pm 49	-36.4
		36.7 \pm 5.8	\pm 12.1	35.2 \pm 5.7	\pm 7.0	37.7 \pm 6.6	\pm 8.7	40.8 \pm 5.8	\pm 37.5
Right	O	278 \pm 52	2.0	266 \pm 15	9.3	257 \pm 18	-10.4	266 \pm 48	6.1
		41.7 \pm 5.5	\pm 5.7	39.7 \pm 3.4	\pm 6.5	38.2 \pm 1.7	\pm 6.4	39.6 \pm 4.8	\pm 24.2
Right	Y	255 \pm 47	1.3	252 \pm 36	9.8	240 \pm 27	-12.4	250 \pm 43	-29.6
		36.9 \pm 6.8	\pm 8.7	37.1 \pm 4.5	\pm 7.8	35.7 \pm 4.0	\pm 11.0	37.1 \pm 5.8	\pm 40.1

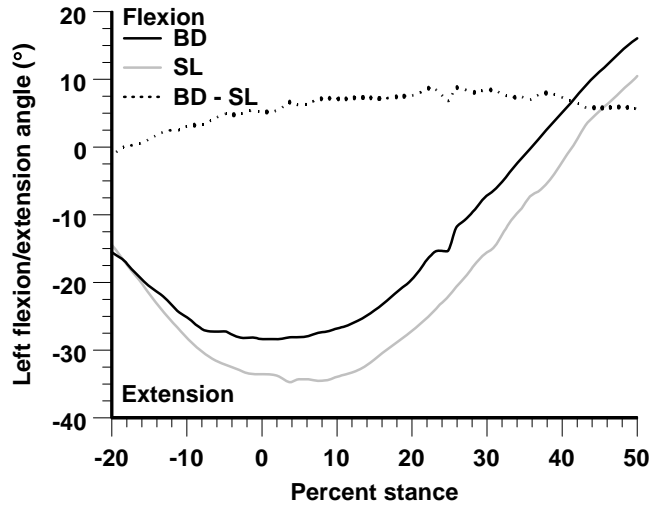


Figure 14. Typical left flexion angle. The left arm in SL trials, which was in extension at heel strike, moved anteriorly in flexion. Thirteen subjects flexed the left arm, and six extended the left upper arm. Ten subjects had no onset.

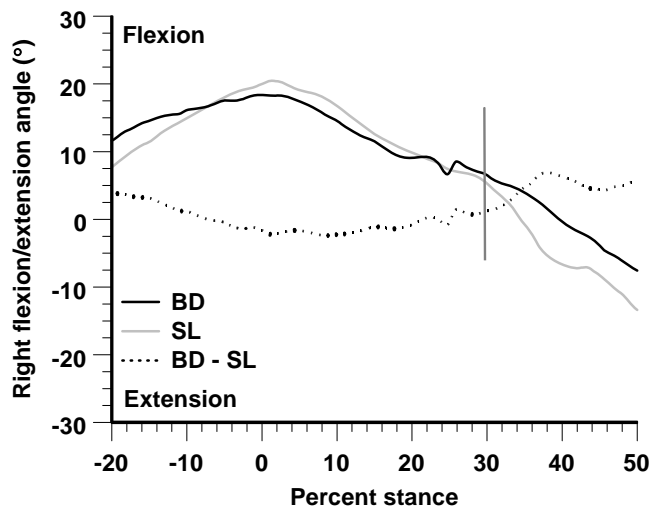


Figure 15. Typical right flexion/extension angle. The vertical line marks the onset of deviation of SL from BD. Seventeen increased the right flexion angle during slip response. Six subjects extended the right arm. Six subjects had no onset.

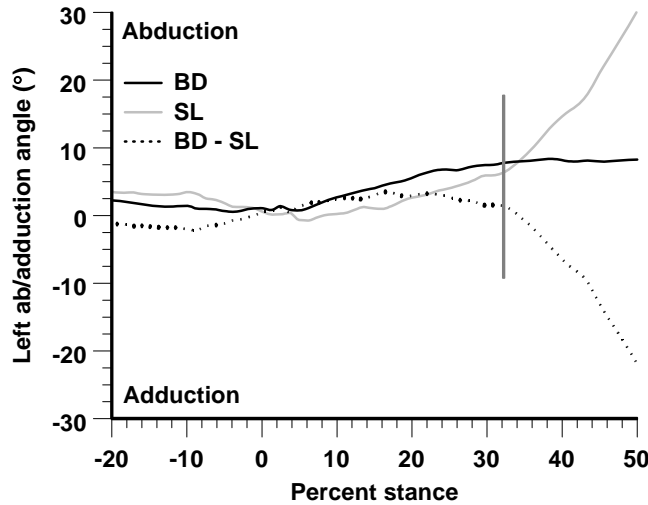


Figure 16. Typical left ab/adduction angle. The vertical line marks the onset of deviation of SL from BD. The upper arm is abducted in response to slip. Twenty-six subjects abducted the left upper arm, and one subject adducted it. Two subjects had no ab/adduction onset. Fifteen subjects continued that response through 50% stance.

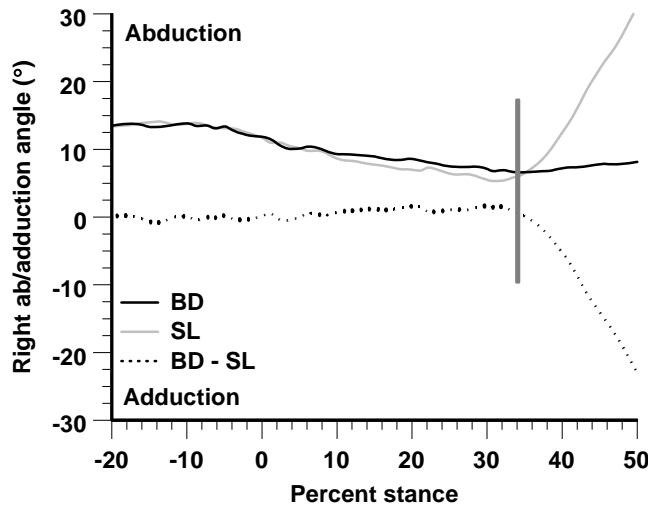


Figure 17. Typical right abduction angle. The vertical line marks the onset of deviation of SL from BD. The right upper arm is abducted in response to slip. Twenty-five subjects abducted the right shoulder, two adducted, and two had no onset. Seven subjects achieved a local peak in response by 50% stance.

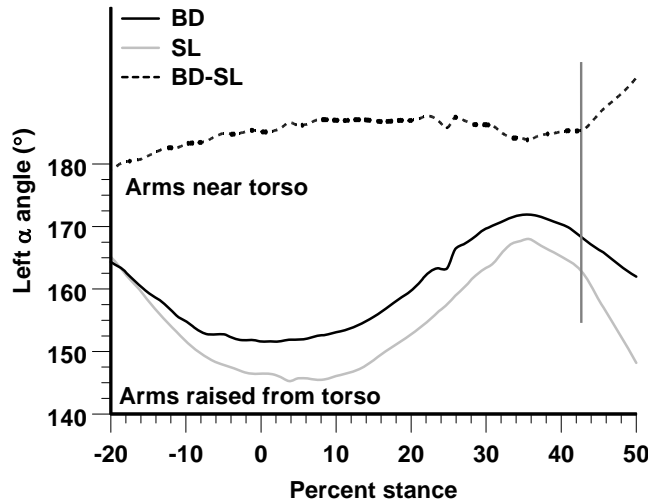


Figure 18. Typical left α angle. The vertical line marks the onset of deviation of SL from BD.

The α angle combines the upward motion of abduction and flexion: At onset, the gray trend declines quickly as the left arm is raised from the torso, which is due mainly to abduction in this case. Eighteen subjects raised the arms from the torso (as in this figure), four lowered the left arm, and seven subjects had no clear onset. A 180° bias was added to the BD-SL trend.

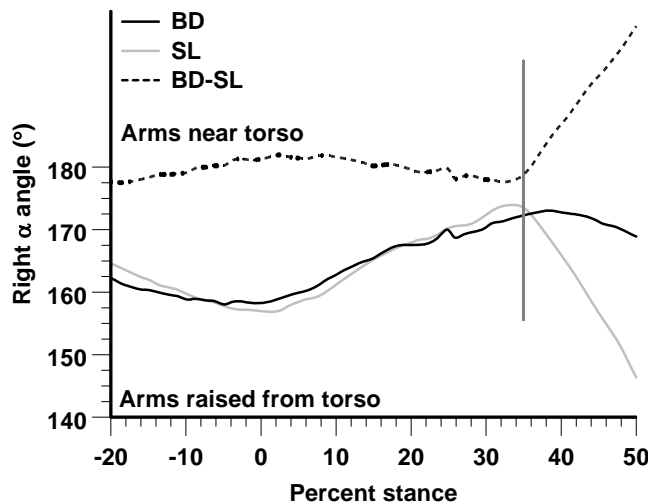


Figure 19. Typical right α angle. The vertical line marks the onset of deviation of SL from BD.

The right α angle decreases as the arms are raised from the torso during slip response. Twenty-one subjects had a similar (arm-raising) response, two subjects lowered the arms, and six subjects had no magnitude change in left α angle. A 180° bias was added to the BD-SL trend.

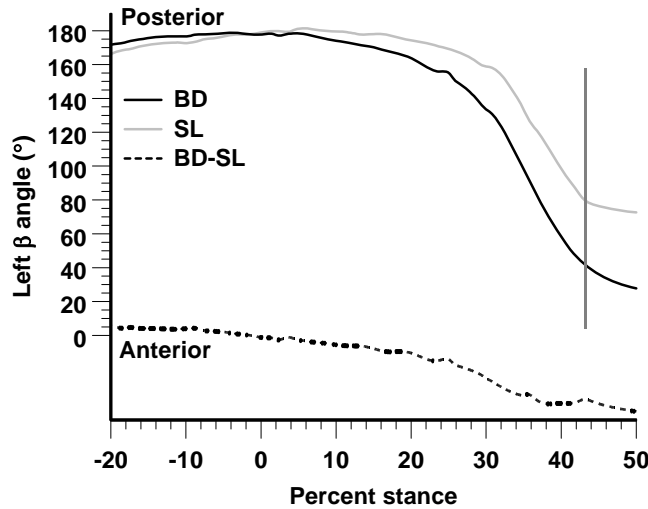


Figure 20. Typical left β angle. The vertical line marks the onset of deviation of SL from BD. The decreasing gray line shows that the subject is moving the arm forward more than left. Fifteen subjects' left β angle decreased (as here), five increased, and nine had no onset. β can change magnitude extremely quickly because of the manner in which it was defined. For instance, if a subject swings the arm from full flexion to full extension in one sweep, passing the elbow next to the torso, β sweeps directly from $\sim 0^\circ$ to $\sim 180^\circ$.

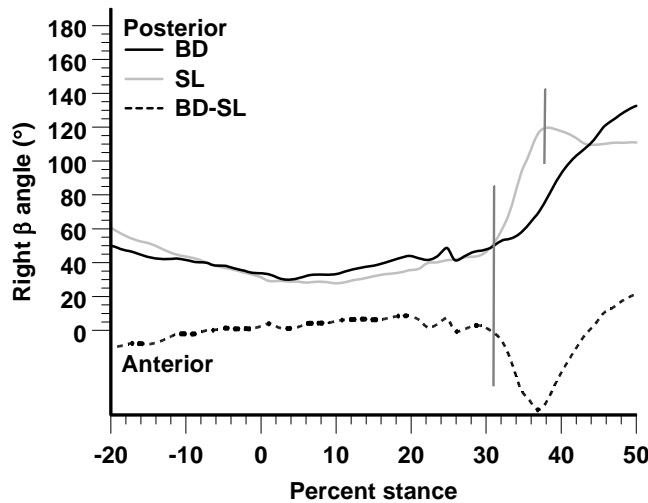


Figure 21. Typical right β angle. The long vertical line marks the onset of deviation of SL from BD, and the short vertical line marks the peak. Five subjects increased right β angle as here, thirteen decreased β angle in slip response, and eleven displayed no response.

In models testing the effect of Age, Severity (Hazardousness, Outcome, and PSV) on magnitude change of shoulder angle, only significant effects on the left arm were found. In

ANOVA models investigating the effect of Hazardousness, Age, and their interaction on magnitude of angle change, Hazardousness only affected left abduction angle significantly (Table 13 and Table 14). Specifically, subjects who experienced hazardous (H) slips increased the left abduction angle more than those with non-hazardous (NH) slips ($p_{\text{Hazardousness}} < 0.05$, Figure 22). In the same statistical models, only change in left flexion angle was significantly affected by Age. Specifically, younger subjects increased left flexion angle more than older subjects in response to slip ($p_{\text{Age}} < 0.05$, Figure 23).

In ANOVA models investigating the effect of Outcome, Age, and their interaction on magnitude of angle change, Outcome only had significant effects on change of left abduction angle and change of left α angle (Table 15 and Table 16). Specifically, subjects whose Outcome was fall (F) rather than recover (R) had greater left shoulder abduction angle ($p_{\text{Outcome}} < 0.05$, Figure 24). Similarly, subjects experiencing Falls had large decreases in α angle, meaning that they raised the arms during slip response ($p_{\text{Outcome}} < 0.05$, Figure 25).

In ANOVA models testing the effect of PSV, Age, and their interaction on magnitude of angle change, only left abduction angle was affected by PSV (Table 17 and Table 18). Specifically, subjects with greater PSV swept the left upper arm through greater abduction angles than subjects with slower PSV ($p_{\text{PSV}} < 0.05$, Figure 26).

Table 13. ANOVA model of Euler angle Magnitudes, Age, and Hazardousness

	Left shoulder angle magnitude		Right shoulder angle magnitude	
	D_{LAflex}	D_{LAabd}	D_{RAflex}	D_{RAabd}
Age	$p < 0.05$	NS	NS	NS
Hazardousness (H/NH)	NS	$p < 0.05$		
Age x Hazardousness	NS	NS		
R^2	0.32	0.23		

Table 14. ANOVA model of spherical angle Magnitudes, Age, and Hazardousness

	Left shoulder angle magnitude		Right shoulder angle magnitude	
	$D_{LA\alpha}$	$D_{LA\beta}$	$D_{RA\alpha}$	$D_{RA\beta}$
Age	NS	NS	NS	NS
Hazardousness (H/NH)				
Age x Hazardousness				
R^2				

Table 15. ANOVA model of Euler angle Magnitudes, Age, and Outcome

	Left shoulder angle magnitude		Right shoulder angle magnitude	
	D_{LAflex}	D_{LAabd}	D_{RAflex}	D_{RAabd}
Age	NS	NS	NS	NS
Outcome (F/R)		p < 0.05		
Age x Outcome		NS		
R^2		0.18		

Table 16. ANOVA model of spherical angle Magnitudes, Age, and Outcome

	Left shoulder angle magnitude		Right shoulder angle magnitude	
	$D_{LA\alpha}$	$D_{LA\beta}$	$D_{RA\alpha}$	$D_{RA\beta}$
Age	NS	NS	NS	NS
Outcome (F/R)	p < 0.05			
Age x Outcome	NS			
R^2	0.29			

Table 17. ANOVA model of Euler angle Magnitudes, Age, and PSV

	Left shoulder angle magnitude		Right shoulder angle magnitude	
	D _{LAflex}	D _{LAabd}	D _{RAflex}	D _{RAabd}
Age	NS	NS	NS	NS
PSV		p < 0.05		
Age x PSV		NS		
R ²		0.27		

Table 18. ANOVA model of spherical angle Magnitudes, Age, and PSV

	Left shoulder angle magnitude		Right shoulder angle magnitude	
	D _{LAα}	D _{LAβ}	D _{RAα}	D _{RAβ}
Age	NS	NS	NS	NS
PSV				
Age x PSV				
R ²				

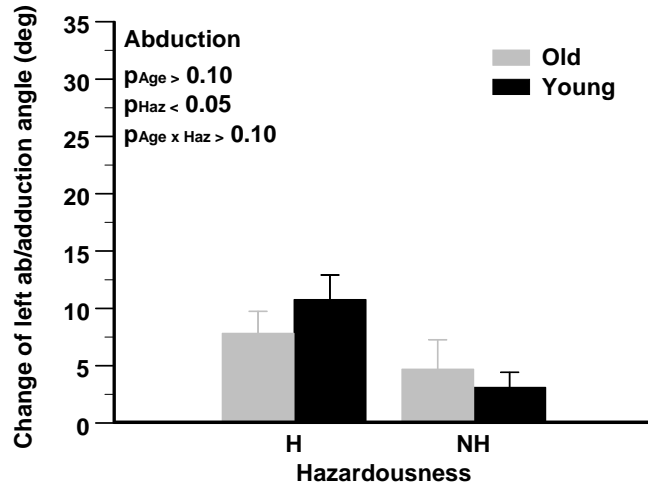


Figure 22. Change of left abduction angle and Hazardousness. ($R^2 = 0.23$) Subjects who experienced hazardous (H) slips also achieved greater changes in left abduction angle. Error bars show standard error.

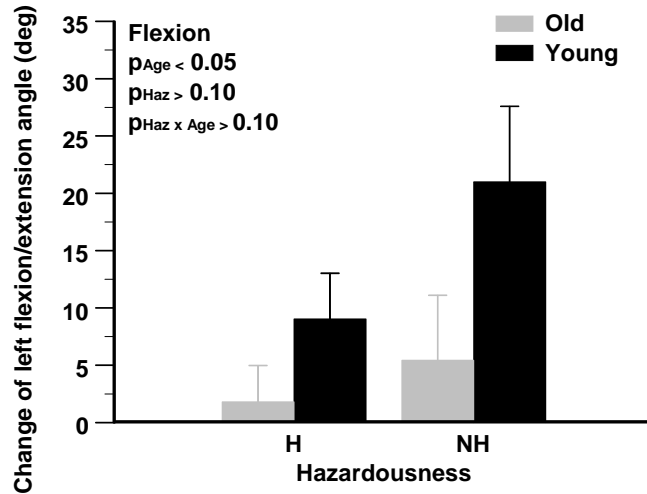


Figure 23. Change of left flexion angle and Hazardousness. ($R^2 = 0.32$) Older subjects showed either small flexion or small extension angles, while young subjects had flexion angles large. Error bars show standard error.

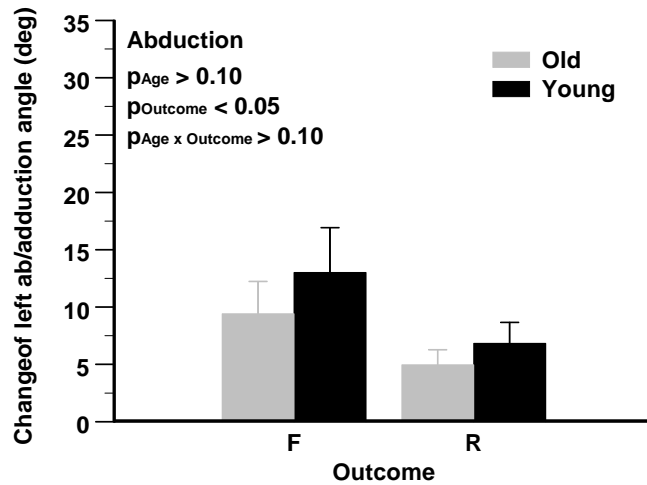


Figure 24. Change of left abduction angle and Outcome. ($R^2 = 0.18$) Subjects whose Outcomes were classified as Falls (F) achieved greater changes in left abduction angle than those with Outcome Recovery (R). Error bars show standard error.

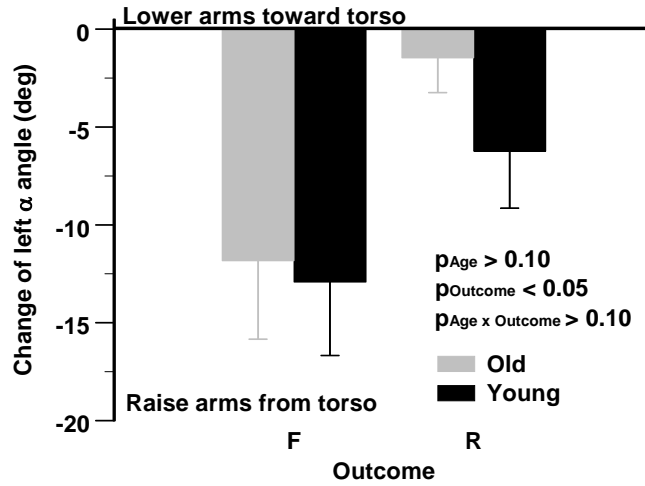


Figure 25. Change of left α angle. ($R^2 = 0.29$) Subjects who fell (F) also tended to raise the arms from the trunk more than those with Outcome Recovery. Error bars show standard error.

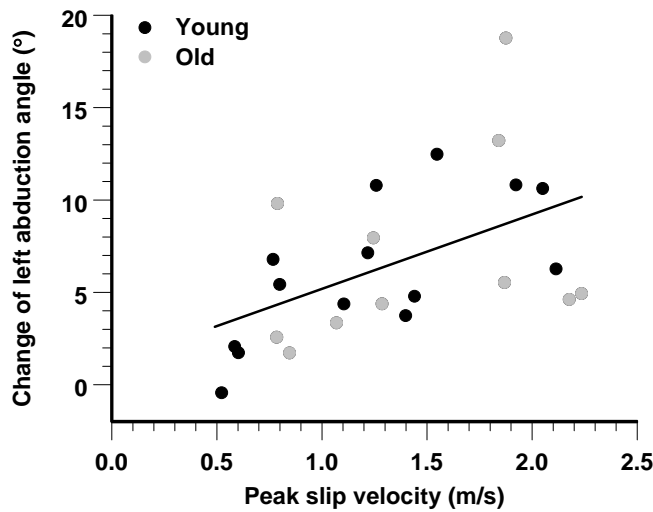


Figure 26. Change in left abduction angle according to PSV. ($R^2 = 0.27$) Subjects with faster PSV abducted the left shoulder more than subjects with slower PSV ($p_{\text{PSV}} < 0.05$).

5.2.2 Shoulder kinetics in slip response: Severity and Age aspects

Responses to slip, i.e. discernible onset in time history trajectory of the moments between 0% and 50% stance, were evident in 69%, 90%, 93%, and 90%, of cases, for left flexion/extension, right flexion/extension, left ab/adduction, and right ab/adduction moments,

respectively. Of the responses, only 20%, 8%, 30%, and 0%, respectively had not reached a peak by 50% stance. Similarly, in left and right summed moment, shoulder response to slip was discernible in 86% and 90% of subjects, respectively. 16% of the left summed shoulder responses were unfinished by 50% stance, and 8% of right summed shoulder response were not complete by 50% stance (Table 19).

Table 19. Quantities of subjects with Onset, and without a conclusive peak value.

Parameter	Have onset pre-50%	Have peak at 50%	PSV(m/s) of subjects without onset
Left flexion moment	20	4	O 1.2, 1.1, 1.3 Y 1.2, 1.4, 0.5, 0.6, 2.1
Right flexion moment	26	2	Y 1.4, 0.5, 0.5
Left abduction moment	27	2	Y 0.5, 0.5
Right abduction moment	26	0	Y 2.1, 0.5, 0.5
Left summed moment	25	4	O 1.1, 1.3 Y 0.5, 0.6
Right summed moment	26	2	Y 2.1, 0.5, 0.5

Left flexion/extension moment was distinguishable in 66% of subjects, and of those, 37% increased moment toward flexion, while the remaining 63% increased moment toward extension (Figure 27). Average onset latencies were 228ms (35% stance) and 230ms (33% stance), for young and old subjects, respectively (Table 20). Right flexion/extension moment was distinguishable in 86% of subjects, and of those, 80% increased moment toward flexion, while the remaining 20% increased moment toward extension (Figure 28). Average onset latencies were 223ms (34% stance) and 215ms (31% stance), for young and old subjects, respectively.

Left ab/adduction moment was distinguishable in 93% of subjects, and of those, 93% increased moment toward abduction, while the remaining 7% increased moment toward adduction (Figure 29). Average onset latencies were 211ms (32% stance) and 197ms (29% stance), for young and old subjects, respectively (Table 20). Right ab/adduction moment was distinguishable in 86% of subjects, and of those, 96% increased moment toward abduction, while

the remaining 4% increased moment toward adduction (Figure 30). Average onset latencies were 194ms (30% stance) and 197ms (29% stance), for younger and older subjects, respectively.

Left summed moment was distinguishable in 86% of subjects, all of whom increased the magnitude of summed shoulder moment (Figure 31). Average onset latencies were 226ms (35% stance) and 212ms (31% stance), for young and old subjects, respectively (Table 20). Right summed moment was distinguishable in 90% of subjects, all of whom increased the magnitude of summed shoulder moment (Figure 32). Average onset latencies were 205ms (31% stance) and 206ms (31% stance), for younger and older subjects, respectively.

Table 20. Mean shoulder onset times and reactions. All quantities given are mean \pm standard deviation.

		Flexion/extension moment		Ab/adduction moment		Summed shoulder moment	
		Onset (ms / %)	Slope (N-m/kg-s)	Onset (ms / %)	Slope (N-m/kg-s)	Onset (ms / %)	Slope (N-m/kg-s)
Left shoulder	O	224 \pm 29 35.3 \pm 5.3	-1.53 \pm 3.07	211 \pm 31 31.7 \pm 5.5	0.64 \pm 1.43	226 \pm 22 34.6 \pm 4.6	2.48 \pm 1.40
	Y	230 \pm 56 33.1 \pm 7.3	-1.04 \pm 1.94	197 \pm 26 29.4 \pm 4.1	2.43 \pm 1.52	212 \pm 31 31.2 \pm 3.8	2.26 \pm 1.24
Right Shoulder	O	223 \pm 37 34.0 \pm 5.9	1.63 \pm 2.05	194 \pm 31 29.6 \pm 4.1	1.50 \pm 1.26	205 \pm 25 31.1 \pm 3.4	2.39 \pm 1.80
	Y	215 \pm 33 30.9 \pm 5.9	1.70 \pm 2.61	197 \pm 32 29.4 \pm 5.6	1.83 \pm 0.72	206 \pm 27 30.9 \pm 4.9	2.61 \pm 1.23

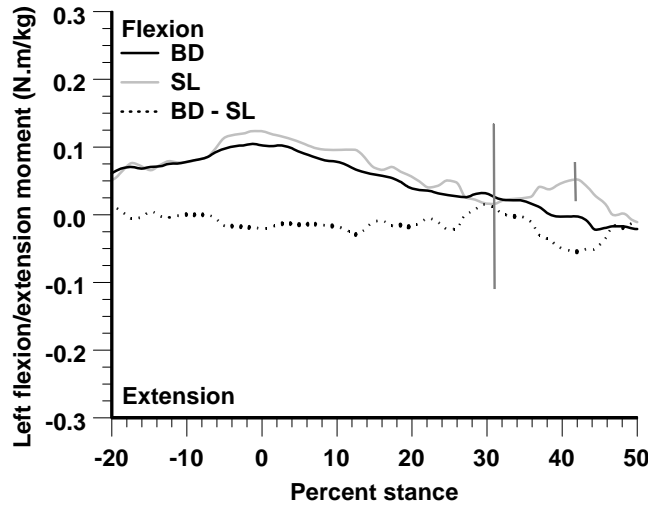


Figure 27. Typical left flexion/extension moment. Left flexion moment normally increased in response to slip, even when kinematics did not reflect this. Onset and peak are illustrated for this case by bars at 31% and 43%, respectively. Seven subjects increased toward flexion moment, twelve subjects increased toward extension moment, and ten had no onset. Of the nineteen subjects with onset, sixteen had peak moment before 50% stance.

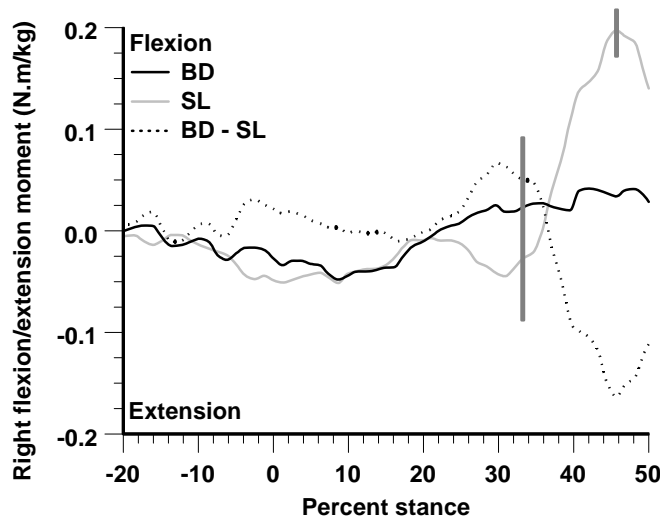


Figure 28. Typical right flexion/extension moment. The shoulder exerts a flexion moment (onset marked by long vertical bar), which peaks prior to 50% stance (marked by short vertical bar). Twenty subjects increased flexion moment, and five increased extension moment. Twenty five subjects had discernible onset, and twenty four of those had pre-50% stance peak.

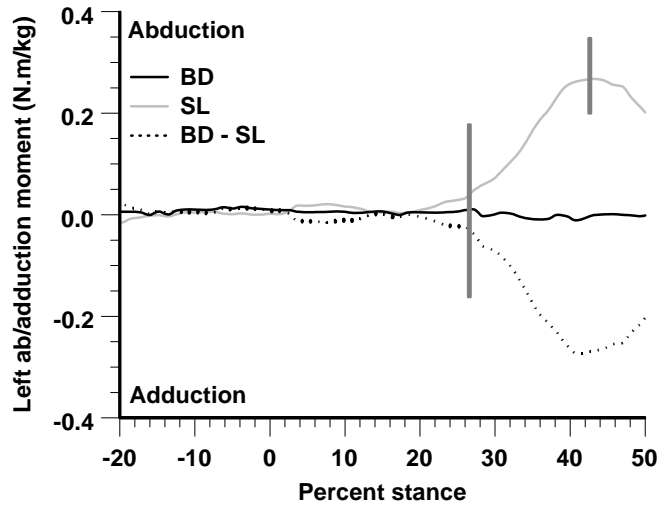


Figure 29. Typical left ab/adduction moment. The long vertical bar indicates onset, and the short vertical bar indicates peak. Twenty five subjects exerted abduction moments and two exerted adduction moments. Twenty seven subjects had onset in response to slip, and twenty five of those subjects had peak moment prior to 50% stance.

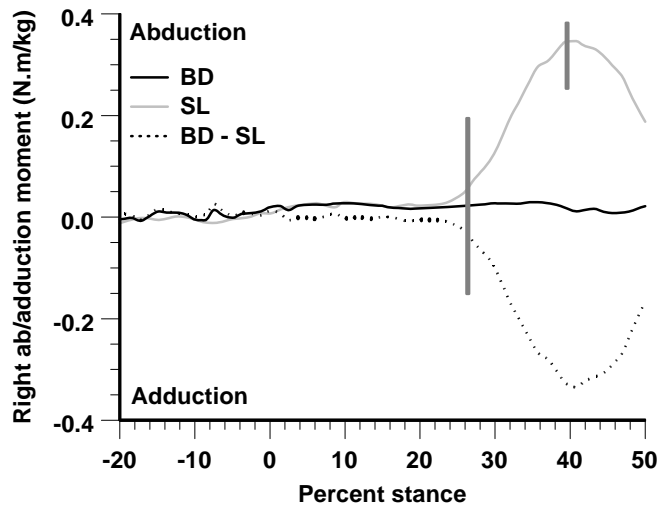


Figure 30. Typical right abduction moment. The long vertical bar indicates onset, and the short vertical bar indicates peak. Twenty four subjects increased abduction moment and one exerted an adduction moment. Four other subjects had no distinguishable onset for this variable.

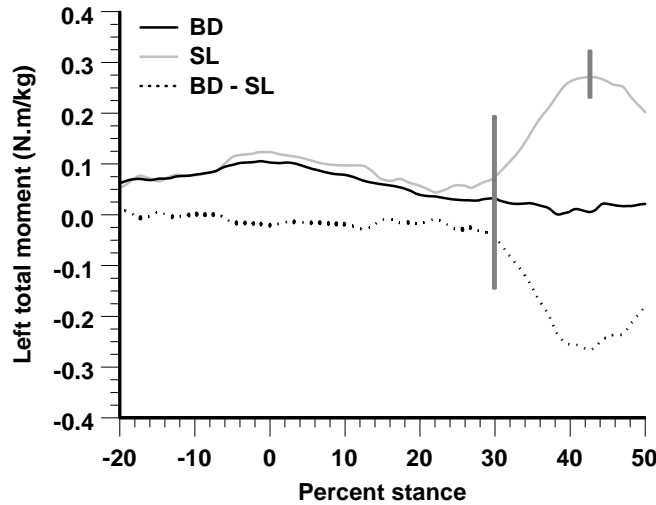


Figure 31. Typical left summed moment. The long vertical bar indicates onset, and the short vertical bar indicates peak. Left summed moment is necessarily positive because it is computed from a sum of squares. The summed moment illustrates that subjects develop general increased moment in the shoulder in response to slip events. Twenty-five subjects showed an increased left summed shoulder moment, and none showed a decrease following slip.

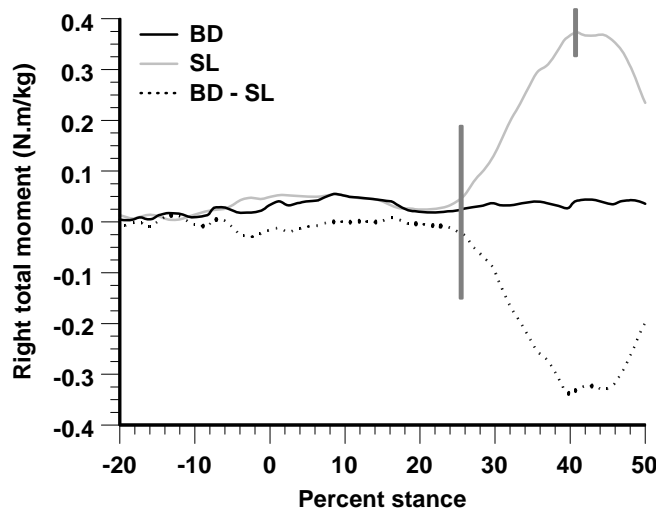


Figure 32. Typical right summed moment. As for the left summed moment, the right summed moment is always positive and illustrates the tendency to increase net shoulder moment magnitude in response to slips. The long vertical bar indicates onset, and the short vertical bar indicates peak. Twenty-six subjects showed an increase in summed shoulder moment, and no subjects had a decrease in shoulder moment.

Onset of shoulder corrective moment

In ANOVA models investigating the effect of slip Severity (PSV, Hazardousness, and Outcome), Age, and their interaction on onset of left/right moment parameter, only Age had a significant effect on the onset of left summed shoulder moment (Table 21 through Table 26). Specifically, in an ANOVA model with fixed effects Age, Outcome, and their interaction, older subjects were shown to have significantly slower onsets of left summed shoulder moment onset than younger subjects ($p_{\text{Age}} < 0.05$, Figure 33). Similarly, in the ANOVA model testing fixed effects PSV, Age, and their interaction on left summed shoulder moment, older subjects were shown to have significantly slower onsets than younger subjects ($p_{\text{Age}} < 0.05$, Table 26).

Table 21. ANOVA model of moment Onset, moment Slope, Age, and Hazardousness. NS indicates no significant effects.

Variable →	Left flex/ext		Right flex/ext		Left ab/adduction		Right ab/adduction	
	Onset	Slope	Onset	Slope	Onset	Slope	Onset	Slope
Age	NS	p < 0.05	NS	NS	NS	p < 0.01	NS	NS
Hazardousness		p < 0.01				p < 0.05		
AgexHazardousness		p < 0.10				NS		
R ²		0.85				0.44		

Table 22. ANOVA model of moment Onset, moment Slope, Age, and Outcome. NS indicates no significant effects

Variable →	Left flex/ext		Right flex/ext		Left ab/adduction		Right ab/adduction	
	Onset	Slope	Onset	Slope	Onset	Slope	Onset	Slope
Age	NS	NS	NS	NS	NS	p < 0.01	NS	NS
Outcome		p < 0.01				NS		p < 0.10
AgexOutcome		p < 0.05				NS		p < 0.05
R ²		0.60				0.30		0.34

Table 23. ANOVA model of moment Onset, moment Slope, Age, and PSV. NS indicates no significant effects.

	Left flex/ext		Right flex/ext		Left ab/adduction		Right ab/adduction	
Model	Onset	Slope	Onset	Slope	Onset	Slope	Onset	Slope
Age	NS	NS	NS	NS	NS	p < 0.01	NS	NS
PSV		p < 0.01				NS		
AgexPSV		NS						
R ²		0.66						

Table 24. ANOVA model of summed moment Onset, moment Slope, Age, and Hazardousness.

Variable →	Left summed moment		Right summed moment	
Model	Onset	Slope	Onset	Slope
Age	NS	NS	NS	NS
Hazardousness				
AgexHazardousness				
R ²				

Table 25. ANOVA model of summed moment Onset, moment Slope, Age, and Outcome

Variable →	Left summed moment		Right summed moment	
Model	Onset	Slope	Onset	Slope
Age	p < 0.05	NS	NS	NS
Outcome	NS	p < 0.05		p < 0.10
AgexOutcome		p < 0.05		NS
R ²	0.27	0.34		0.23

Table 26. ANOVA model of summed moment Onset, moment Slope, Age, and PSV.

Variable →	Left summed moment		Right summed moment	
Model	Onset	Slope	Onset	Slope
Age	p < 0.05	NS	NS	NS
PSV	NS			
Age x PSV		p < 0.05		
R ²	0.29	0.29		

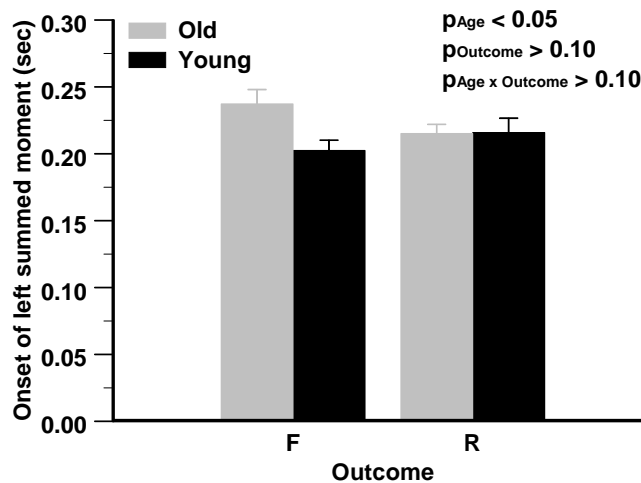


Figure 33. Onset of left summed moment stratified by Age group and Outcome. ($R^2 = 0.27$) Older adults had later onsets of summed shoulder moments than younger adults. Error bars show standard error.

Slope of shoulder moment

In ANOVA models investigating the effect of Severity (PSV, Hazardousness, and Outcome), Age, and their interaction on right shoulder moment generation, only the generation rate of right ab/adduction moment were significantly affected by the interaction *Age x Outcome* (Table 21 through Table 26, Figure 34). Specifically, older subjects with outcome recovery had slower right abduction moment generation rates than older subjects with outcome fall ($p_{Age \times Outcome} < 0.05$, Table 22). A trend suggests that those with outcome fall generated right abduction angle faster than those with outcome recovery ($p_{Outcome} < 0.10$, Table 22). There is also a trend

suggesting that those who slowly generate right summed moments tend to recover rather than fall ($p_{\text{Outcome}} < 0.10$, Table 25).

In ANOVA models investigating the effect of Severity (PSV, Hazardousness, and Outcome), Age, and their interaction on left shoulder moment generation, several significant effects on flexion/extension, ab/adduction, and summed moment generation rate were found (Table 21 through Table 26). Specifically, a strong negative correlation between PSV and left flexion moment generation rate was found ($p_{\text{PSV}} < 0.01$, $R^2 = 0.66$, Figure 35). Likewise, subjects experiencing hazardous slips (i.e., $\text{PSV} > 1.0$ m/s) generated increasing left extensor moments. Those experiencing non-hazardous slips (i.e., $\text{PSV} < 1.0$ m/s) generated increasing left flexor moments ($p_{\text{Hazardousness}} < 0.01$, Figure 36). Older subjects generated moments tending more toward extension, while younger subjects generated moments that tended toward flexion ($p_{\text{Age}} < 0.05$, Figure 36). Examining left flexion/extension moment generation rate in terms of slip outcome, those who fell generated greater extensor moments in the left shoulder than those who recovered ($p_{\text{Outcome}} < 0.01$, Figure 37). Older subjects with outcome recovery generated increasing left flexion moments, while older subjects with Outcome Fall generated increasing extension moments. Younger subjects who recovered tended to generate extension moments significantly slower than older adults experiencing a fall ($p_{\text{Age} \times \text{Outcome}} < 0.05$, Figure 37).

The only Severity measure affecting left abduction moment generation rate was Hazardousness, which showed that subjects who experienced hazardous slips generated left abduction moments more slowly than subjects with non-hazardous slips ($p_{\text{Hazardousness}} < 0.05$, Figure 38). Older subjects generated left abduction angle significantly slower than younger subjects ($p_{\text{Age}} < 0.01$, Figure 38, Table 21, Table 22, and Table 23).

Only PSV and Outcome had significant effects on left shoulder summed moment generation rate. Specifically, older subjects with low PSV values generated left shoulder moments slowly, while older subjects with fast PSV generated left shoulder moments quickly, and neither young group (fall or recovery outcome) was significantly different than either old fall group or old recover group ($p_{\text{Age} \times \text{PSV}} < 0.05$, Figure 39). There was a significant effect between subjects who increased their left summed shoulder moments very quickly and those who fell ($p_{\text{Outcome}} < 0.05$, Figure 40). Older subjects with Outcome Recovery developed summed left shoulder moments significantly slower than older subjects who experienced Falls. Such an effect was not evident among younger subjects ($p_{\text{Age} \times \text{Outcome}} < 0.05$, Figure 40).

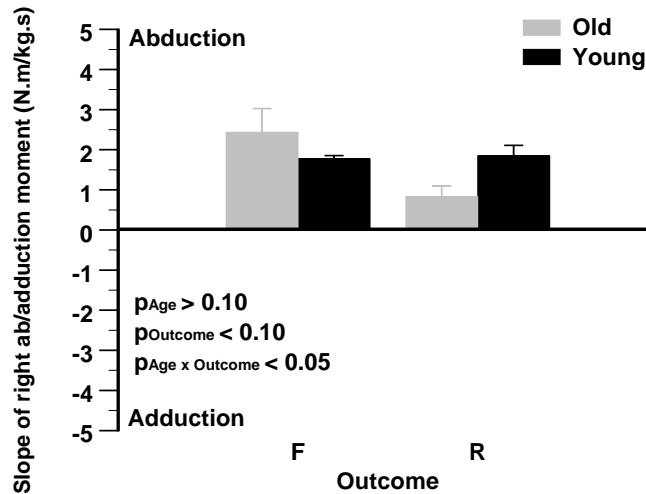


Figure 34. Right abduction moment generation rate stratified by Age group and Outcome. ($R^2 = 0.34$) Older subjects with Outcome Recovery had slower right abduction moment generation rates than older subjects with Outcome Fall. Error bars show standard error.

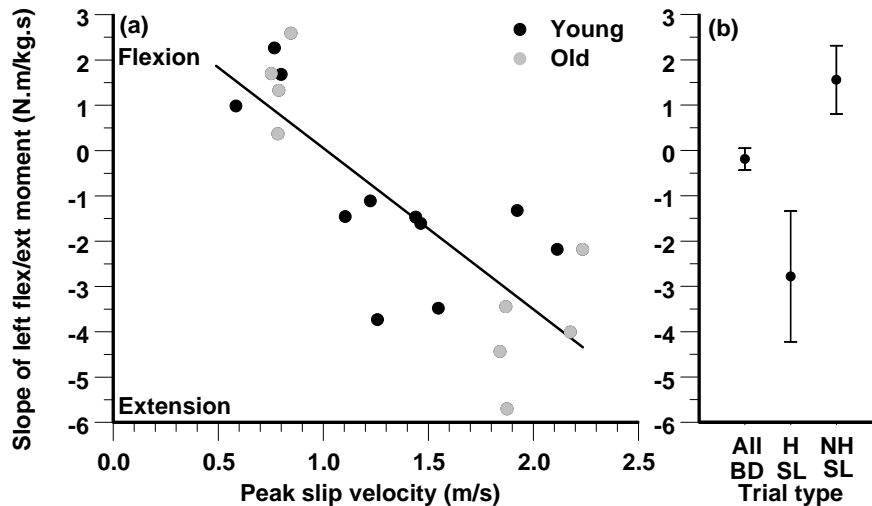


Figure 35. Flexion moment generation rate in the left shoulder compared to PSV. (a) Slope of left should moment generation rate in slip trials ($R^2 = 0.66$, $p_{PSV} < 0.01$). 9 subjects (3 older and 6 younger) had no left flexion moment onset; therefore, the table above has only 20 data points. Subjects with slower PSV tended to also generate increasing flexion moment and those with faster PSV tended to generate increasing extension moments. Age had no significant effect on this relationship ($p_{Age} > 0.10$). (b) Mean left flexion/extension moment generation rate calculated in (1) All dry trials, (2) Hazardous slip trials, and (3) Non-hazardous slip trials. The Non-hazardous group differed significantly during slip trials from the group of all subjects in dry trials ($R^2 = 0.87$, $p_{Haz} < 0.01$). The Hazardous group differed significantly during slip trials from the group of all subjects in dry trials ($R^2 = 0.83$, $p_{Haz} < 0.01$). Error bars illustrate standard deviation.

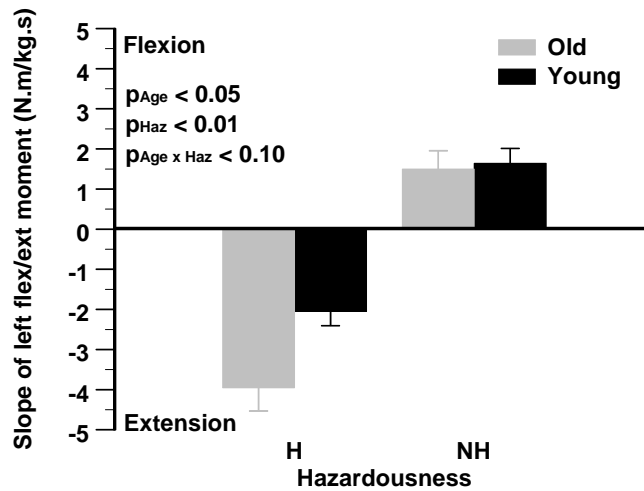


Figure 36. Left flexion moment generation rate stratified by Age group and Hazardousness. ($R^2 = 0.85$) Subjects with hazardous (H) slips increased left extensor moments, and those with non-hazardous slips (NH) generated increasing left flexion moments. Older subjects generated moments tending more toward extension, while younger subjects generated moments that tended toward flexion. Error bars show standard error.

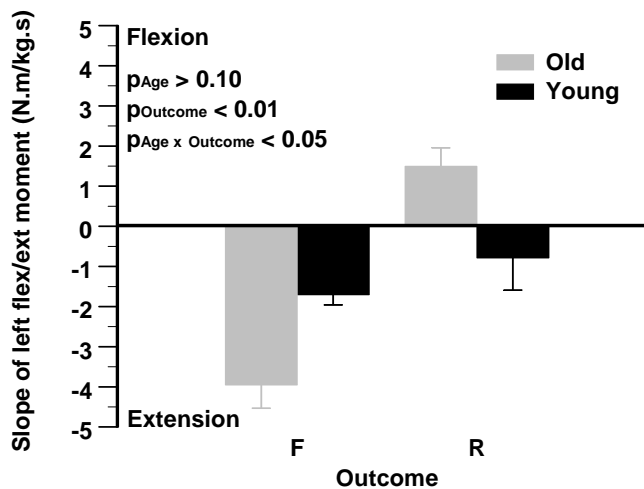


Figure 37. Left flexion moment generation rate stratified by age group and outcome. ($R^2 = 0.60$) Fallers generated extensor moments in the left shoulder faster than those who recovered. Older subjects with Outcome Recovery generated increasing left flexion moments, while older subjects with Outcome Fall generated increasing extension moments. Younger subjects who recovered tended to generate extension moments significantly slower than older adults experiencing a fall.

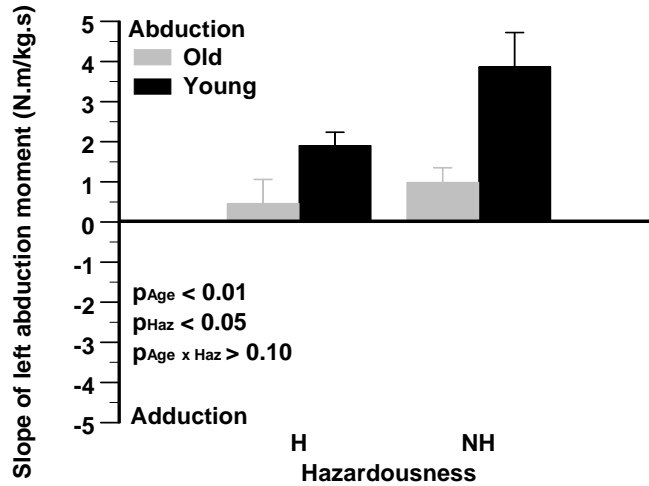


Figure 38. Left shoulder abduction moment generation rate stratified by age group and Hazardousness. ($R^2 = 0.44$) Subjects with non-hazardous slips generated left abduction moments faster than those who experienced hazardous slips, and older adults generated smaller rates of increase in left abduction moment than younger subjects did. Error bars show standard error.

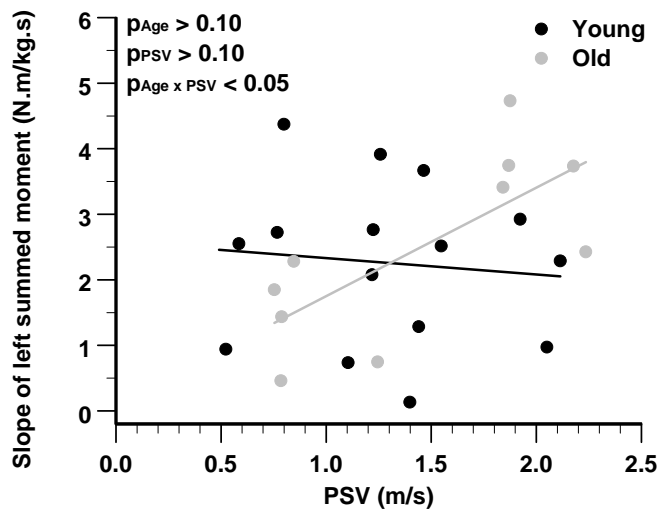


Figure 39. Slope of left summed shoulder moment compared to PSV, stratified by Age. ($R^2 = 0.29$) Older subjects who have slow PSV values generated left summed shoulder moments gradually, while older subjects who have fast PSV values generate left summed moment quickly. Younger subjects showed no such trend.

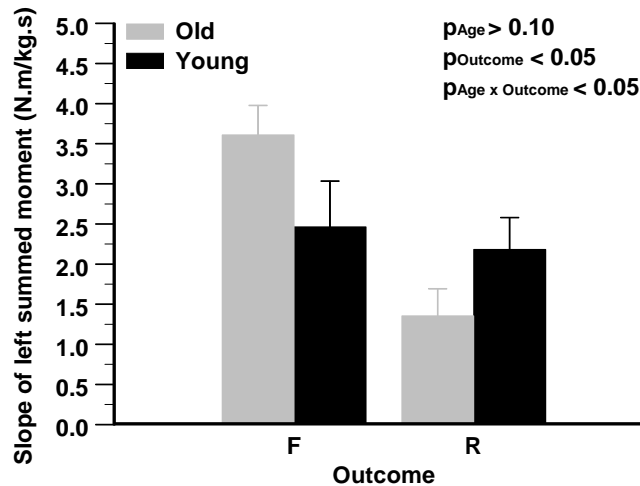


Figure 40. Summed left shoulder moment generation rate stratified by age group and outcome. ($R^2 = 0.30$) Subjects who increased their left shoulder moments very quickly tended also to fall. Older subjects with outcome recovery developed summed left shoulder moments significantly slower than older subjects who experienced falls. Such an effect was not evident among younger subjects. Error bars show standard error.

5.2.3 Comparison of shoulder and leg response timing

Left shoulder reactive flexion moment occurs significantly later than both hip and knee flexion moment in response to unexpected slip (Figure 41).

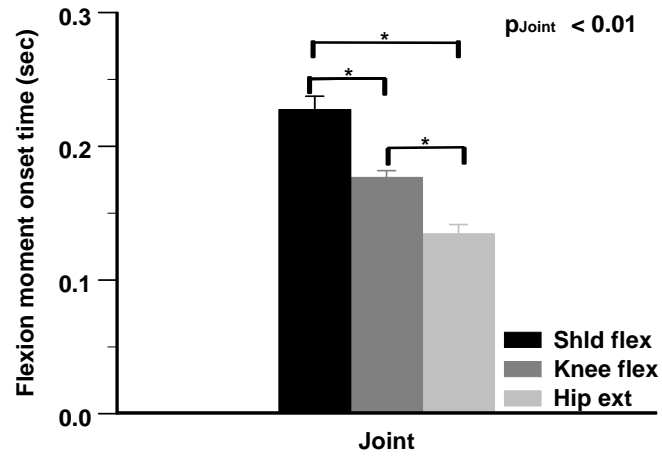


Figure 41. Comparison of reactive moment onsets in the left shoulder, knee, and hip, averaged across all subjects. ($R^2 = 0.72$) Subjects initiated left shoulder flexion moment significantly later than both hip flexion moment and knee flexion moment. Error bars show standard error. (* $p < 0.05$)

5.3 HEAD ACCELERATION

5.3.1 Head COM motion during ordinary gait

Typical data of head motion during BD walking trials (Figure 42) shows cyclic head motion during gait. The head COM moves up and down with the greatest frequency and highest velocity and acceleration. Peaks in the vertical position occur during single-support, and local minima occur at double support (Figure 42a). In the M/L direction the head rocks in the direction of the stance leg following each successive heel strike (Figure 42d). In the A/P direction, the head moves steadily forward with relatively constant velocity (Figure 42g, h, i). In general, maxima or minima of the M/L acceleration curve do not coincide with maxima or minima of the vertical acceleration curve.

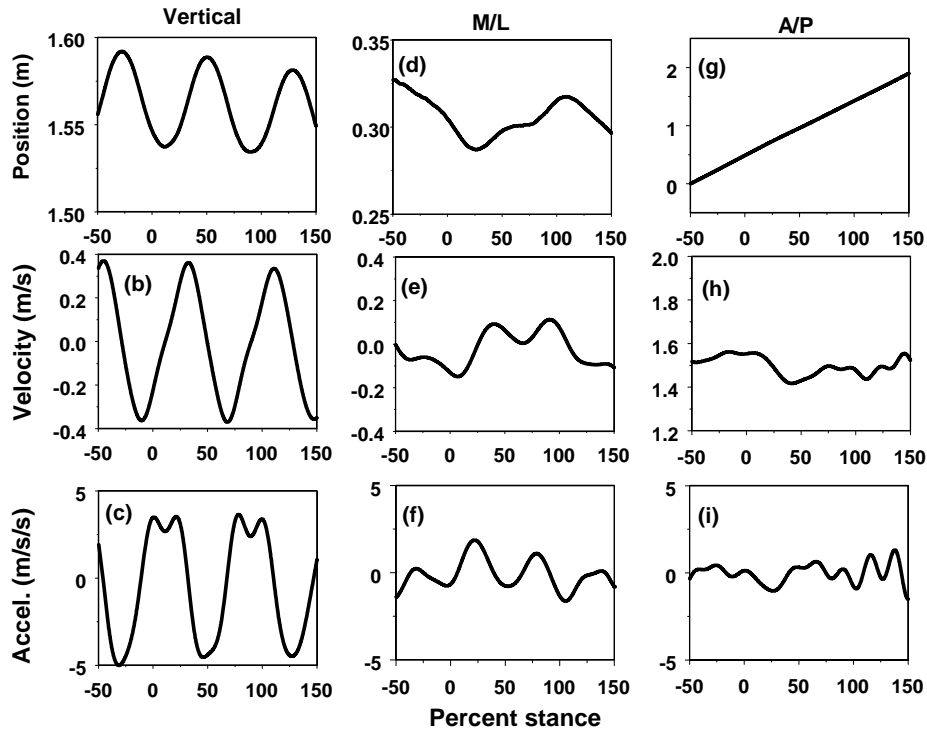


Figure 42. Typical normal HCOM trajectories. Trajectories for one typical subject through the course of an entire BD trial. (Positive = Up/Right/Forward; Negative = Down/Left/Backward) *Vertical* (a, b, c) The head COM moves up and down with the greatest frequency and highest velocity and acceleration. Peaks in the vertical position occur during single-support, and local minima occur at double support. *Mediolateral* (d, e, f) In the M/L direction the head rocks in the direction of the stance foot following each successive heel strike (d, e, f). *Anteroposterior* (g, h, i) In the A/P direction, the head moves steadily forward with relatively constant velocity. In general, maxima or minima of the M/L acceleration curve do not coincide with maxima or minima of the vertical acceleration curve.

5.3.2 Head COM motion during unexpected slips

Head COM position during slip (Figure 43) was marked by a clear vertical drop and lateral deviation toward the slipping (left) foot in the SL trial (~20% stance) but only later in the trial was a decline in forward progression visible (~40% stance) between BD and SL trials. In vertical acceleration, this more rapid downward trend was observed between 0% and 15% stance, whereas a deviation in M/L head acceleration varied widely, from about 0% to 30% stance. A/P acceleration variation was similar to that in the M/L direction; the head accelerated first backward before declining in acceleration.

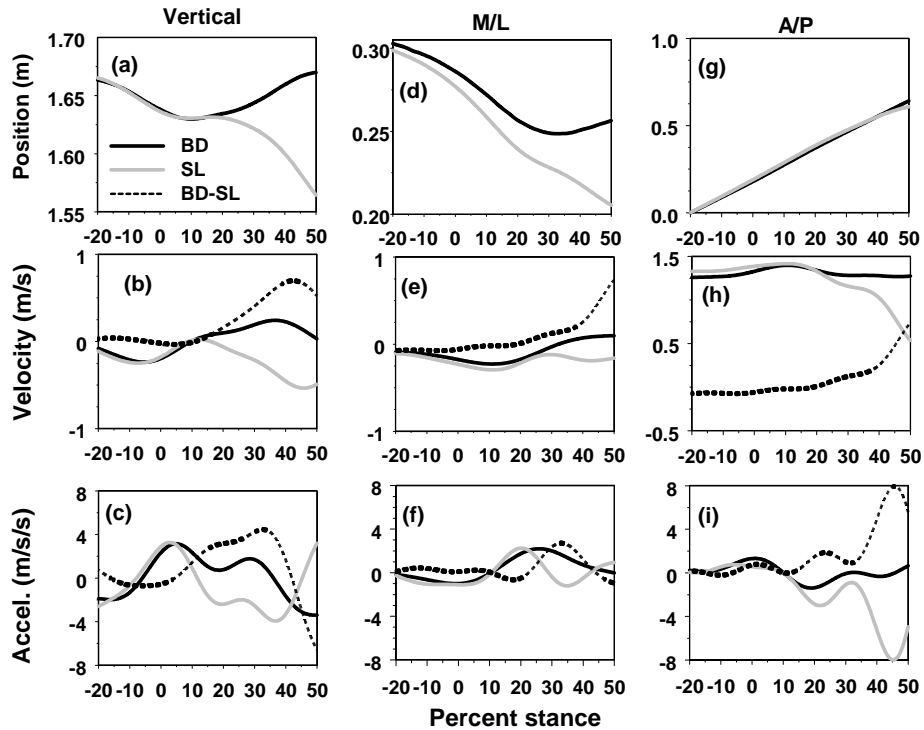


Figure 43. Comparison of dry/slippery trials. (Positive = Up/Right/Forward; Negative = Down/Left/Backward) In the position graph, only BD-SL is omitted to allow better view of BD and SL trials. PSV in this case is 1.4m/s. *Vertical* (a,b,c) In the acceleration graph, the vertical gray line marks the onset of vertical head acceleration, where the head acceleration in the SL trial peaks after LHS. Little difference was distinguishable between the BD and SL traces before 20% stance in the position graph. The difference is noticeable in the velocity graph only slightly earlier (~15% stance). *Mediolateral* (d,e,f) As the subject slips on the left foot, the head COM moves left, indicated by a decrease in head position. In the velocity and acceleration graphs, no major difference between BD and SL trials occurs until late in the trials. Head velocity in SL trials continues leftward, in contrast to BD trials, where velocity increases to the right. Head acceleration is pointed distinctly to the left as the slip proceeds. *Anteroposterior* (g,h,i) In the position graph, BD and SL plots progress steadily forward together until about 40% stance. In the velocity graph, slight differences in the COM path are highlighted by the first derivative. The acceleration graph shows that as the subject slips, the head COM accelerates backward before returning to almost constant velocity. Deviation of BD and SL A/P acceleration traces was highly variable and often indiscernible because the two traces did not match approaching LHS.

Onset of vertical head acceleration has a significant effect on onset of net left shoulder moment when controlled for Outcome ($p_{tAz} < 0.05$, Table 27). This relationship is a positive correlation between onset of vertical acceleration of the head and onset of the left summed shoulder moment, but this relationship is weak ($R^2 = 0.29$, Figure 44). Onset of vertical head acceleration had no significant effect on right summed shoulder moment onset (Table 27).

Table 27. Summary of statistical results concerning head motion. t_{AZ} has a significant effect on t_{LMsum} when controlled for Outcome (* indicates $p < 0.05$). The column ΔR^2 shows the fraction of ANOVA Model 3 that was not explained by model 1; that is, t_{AZ} accounts for 16% of the fit in ANOVA Model 3. The head acceleration variable t_{AZ} was found to have no significant effect on the movement on the right arm. t_{AZ} had a significant effect on t_{LMsum} (onset of summed left shoulder moment).

Dependent variables	Model 1 Outcome (F/R)	Model 2 t_{AZ}	Model 3 Outcome, t_{AZ}	ΔR^2 of M3-M1
Left shoulder moment onset	$R^2 = 0.06$	$R^2 = 0.13$	$R^2 = 0.29$ (t_{AZ}^*)	0.16
Right shoulder moment onset	$R^2 = 0$	$R^2 = 0$	$R^2 = 0$	0

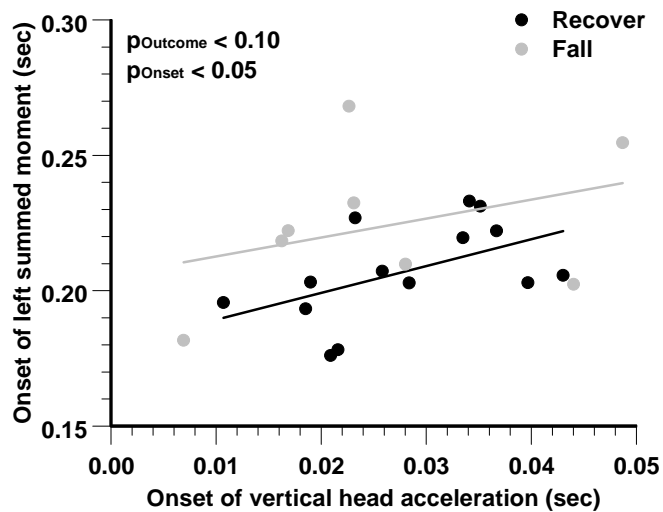


Figure 44. Onset of left summed shoulder moment vs. onset of vertical acceleration of the head COM. ($R^2 = 0.29$) Subjects who fell also tend to have later onset of left summed shoulder moment (t_{LMsum}) than those who recovered. Subjects with earlier head acceleration (t_{AZ}) tended to have earlier left shoulder moment onset.

5.4 EFFECT OF ARM DYNAMICS ON WHOLE BODY COM MOTION

θ trajectories indicate that in dry conditions, after heel strike, the COM rises and advances anteriorly with respect the BOS (Figure 45). Typically, subjects who recover maintain similar trajectories in dry and slippery trials. The COM advances anteriorly and superiorly with respect to the BOS in SL as in BD, as shown by a monotonic increase in θ . In outcomes considered falls, typically the subject's θ does not continue to rise much after heel strike, meaning that the BOS remains to the subject's anterior, and that the COM does not become further elevated (Figure 46, [7]).

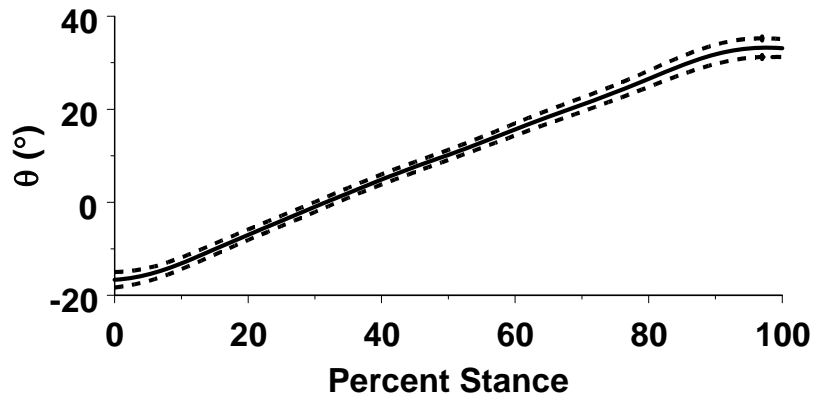


Figure 45. Ensemble average of θ across dry trials. The trajectory of θ illustrates the path of the COM with respect to the BOS. After heel strike, the COM rises and advances anteriorly with respect the BOS. The dashed lines depict \pm one standard deviation [7].

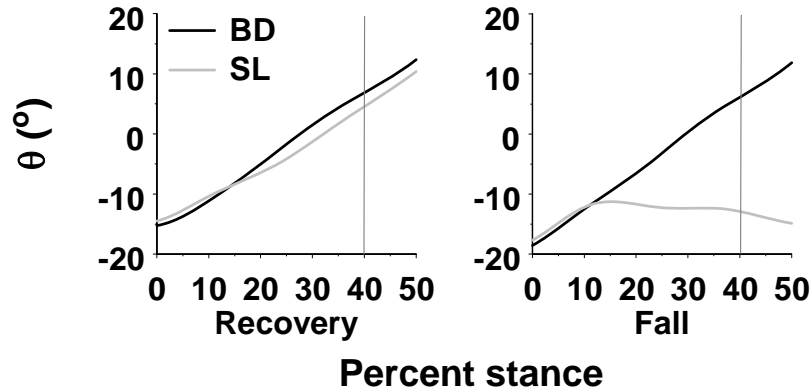


Figure 46. Typical dry/slippy θ trajectories for one recovery and one fall. The subject who recovers maintains similar trajectories in dry and slippery trials: The COM advances anteriorly and superiorly with respect to the BOS in SL as in BD. In the fall, the subject's θ does not continue to rise much after heel strike, meaning that the BOS remains to the subject's anterior, and that the COM does not become further elevated. The gray line marks 40% stance, the instant for which θ_{40} is computed [7].

There was a negative correlation between the left shoulder moment generation rate and the stability measure θ_{40} ($p_{\text{SLMflex}} < 0.01$, Figure 47). Those who exerted extension moments had much lower θ values in the BD trial than in the SL trial, and those with increased flexion moments were likely to have similar θ values in BD and SL trials.

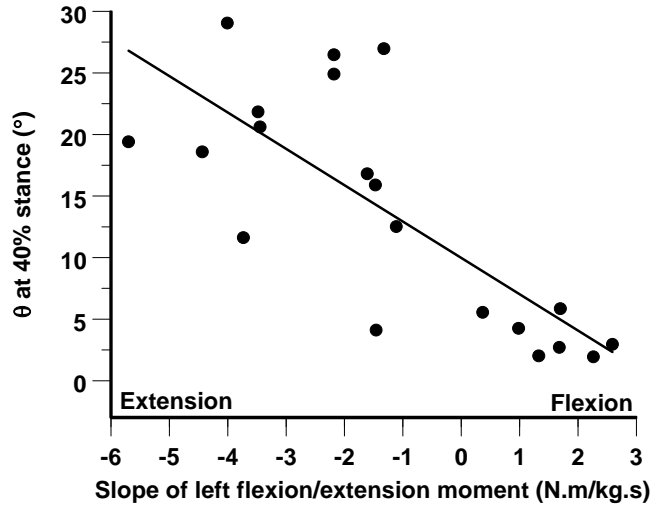


Figure 47. Effect of slope of left flexion moment (S_{LMflex}) on θ_{40} . ($R^2 = 0.58$) There is a negative correlation between θ_{40} and S_{LMflex} ($p_{S_{LMflex}} < 0.01$). Those who exerted extension moments had much lower θ values in the BD trial than in the SL trial, and those with increased flexion moments were likely to have similar θ values in BD and SL trials. Age had no effect on θ_{40} ($p_{Age} > 0.10$).

The interaction $Age \times t_{LMsum}$ was found to have significant effects on θ_{40} and θ_{max} ($p_{Age \times t_{LMsum}} < 0.05$, Figure 48, Table 28). Older subjects with early onset of left summed shoulder moment are more stable in slips, while subjects with later onset of left summed shoulder moments are less stable in slip response. However, younger subjects who had earlier onsets of left shoulder moment became more unstable than young subjects with later onset.

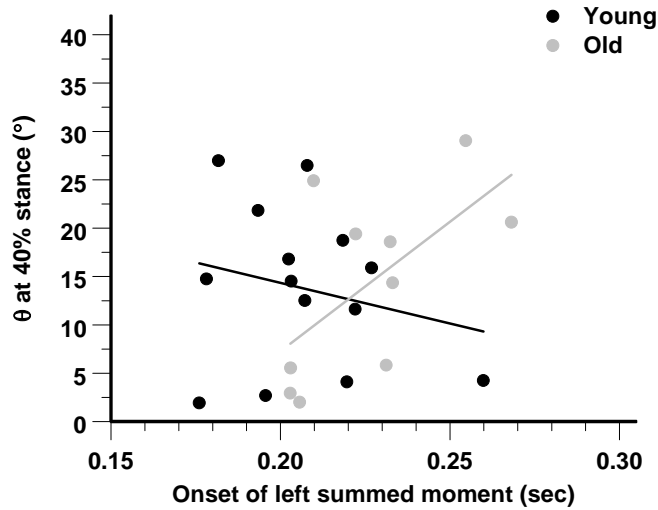


Figure 48. θ_{40} versus onset of left summed moment. ($R^2 = 0.21$) The interaction $Age \times t_{LMsum}$ has a significant effect on θ_{40} , a measure of stability of the COM. Older subjects with early left moment onsets had lower θ_{40} , and older subjects with later left shoulder moment onsets had higher θ_{40} . The opposite was true for younger adults: Those with early left shoulder moment onsets achieved higher θ_{40} , while those with later onsets achieved lower θ_{40} ($p_{Age \times t_{LMsum}} < 0.05$).

Table 28. ANOVA models used concerning whole body COM motion and onset of left summed shoulder moment. Only the interaction $Age \times t_{LMsum}$ had significant effects on the difference in θ between BD and SL trials.

Independent variables	Dependent variable
	θ_{40}
Age	$p > 0.10$
t_{LMsum}	$p > 0.10$
$Age \times t_{LMsum}$	0.0412
R^2	0.21

6.0 DISCUSSION

6.1 SUMMARY OF FINDINGS

Although arm responses were bilateral, only left shoulder biomechanics, specifically moment generation rates, spherical elevation angle, and abduction angle were positively correlated with slip severity. Left shoulder responses were triggered later than left hip and knee responses. Delayed shoulder moment onsets, slower abduction moment generation rate, and reduced range of motion were found in older adults compared to their younger counterparts. Aim 2 results indicated a weak but statistically significant positive relationship between the timing of the slip-initiated downward head acceleration and the onset of the left shoulder flexion/extension moment (when slip severity was controlled in the analysis). In Aim 3, increased left shoulder flexion generation rate correlated with decreased COM perturbation.

6.2 ARM REACTIONS TO SLIPS

6.2.1 Shoulder kinematics and kinetics in slip response

In this study, arm movements were found to be correlated with slip severity but only on the left side, ipsilateral to the slipping foot. The left-right asymmetry implies that arms are at least partially involved in stabilizing the perturbed body. Previous studies have suggested that arm movements are protective in nature, e.g. reaching a hand rail for support or protecting the upper body from impacting the floor [3,10,22,24]. In our experimental setup, this would suggest that the arms would move downward to brace for impact with the floor. Indeed, extension of the ipsilateral arm was seen but only in severe slips, and this may stem from a fall-breaking strategy.

From a more holistic standpoint, past findings and our findings can provide unified support of Roberts' proposal that postural responses include a sweeping response of the arms for inertial effects, and later, a fall-breaking reaction [37]. The role of the contralateral (right) shoulder was unclear in this study. External perturbation elicited some response on the right side of the body, but overall differences in the right limb between dry and slip trials were small. It can be argued that the right arm was already near full flexion at the time of slip initiation, shortly after left heel contact on the slippery floor, rendering increased flexion useless.

Left shoulder activity was moving in its intended direction based on a qualitative examination of the joint power data. (Joint power is the product of joint angular velocity and moment). In the sagittal plane:

- 67% of subjects concentrically contracted shoulder flexors (exerted a flexion moment and produced a flexion movement)
- 29% eccentrically contracted shoulder extensors (exerted an extension moment but produced a flexion movement)
- 4% eccentrically contracted shoulder flexors (exerted a flexion moment but nonetheless produced extension movement)
- 0 concentrically contracted shoulder extensors (exerted extension moment and produced an extension movement)

In the frontal plane:

- 70% of subjects concentrically contracted shoulder abductors (exerted an abduction moment and produced an abduction movement)
- 15% eccentrically contracted shoulder abductors (exerted an abduction moment but nonetheless produced adduction movement)
- 11% eccentrically contracted shoulder adductors (exerted an adduction moment but produced abduction movement)
- 4% concentrically contracted shoulder adductors (exerted adduction moment and produced an adduction movement)

In summary, in about 25% of shoulder movements, the subjects' arms moved in an unintended direction, whereas about 75% of the motions successfully followed their intended direction. Subjects controlled their arm movements in response to slips.

6.2.2 Age effects in shoulder kinematics and kinetics during slips

Older and younger subjects differed significantly in the direction of shoulder moments generated in response to slip: Older subjects extended rather than flexed the ipsilateral shoulder joint. These aging-related differences can be interpreted in two ways: (1) older subjects use their arms to achieve different goals in slip response (e.g., attempting to prevent an impact of the upper body onto the floor) than younger subjects (e.g., attempting to recover balance by changing the body's moment of inertia or by shifting COM position); (2) Both younger and older adults attempt to achieve the same goal, i.e. recovering balance, by using their arm, but older adults are not successful, misdirecting their arm movements. Also, older adults had significantly later left summed shoulder moment onset than younger adults.

In general, our findings compare well with previous research. Tang and Woollacott reported ineffective postural responses in older adults (ages 70-87) consisting of longer trunk muscle latencies and smaller-magnitude EMG bursts. These authors also noted that older subjects raised the arms to move the COM forward, while we found that older adults extended the arms [41].

Allum and colleagues found that young adult reactions to perturbed stance were characterized by earlier, stronger reactions than in elderly adults, and younger subjects' reactions were closely modulated by perturbation direction. In agreement with our findings, Allum and colleagues reported differences in the direction of arm movements in young and older adults [3]. Specifically, arm movement was in the direction of trunk roll in younger adults, but initial trunk roll was opposite in elderly subjects and young subjects [3].

6.2.3 Comparison of shoulder and leg response timing

We expected to find that the shoulder moment onset would be comparable to moment onset of the knees and hips, but the opposite was found to be true: Left shoulder flexion moment onset was significantly later than knee and hip moments. The hypothesis was based on findings by several authors that shoulder and arm muscle onsets in response to postural perturbation were detectable by EMG at approximately the same time as leg muscle onsets. Early onset of shoulder muscles was found similar to early leg muscle onset in perturbed stance [24].

Simultaneous initial muscle onsets (of about 80ms) in the arms and legs were observed in some subjects following underfoot gait disturbance, or stimulation of the tibial nerve [16]. Marigold et al found that both right and left deltoid had onset simultaneously with leg muscles (at approximately 140-150ms) during gait; however, no substantial changes in arm kinematics occurred until 250-300ms after heel strike [23]. In contrast to these findings, Romick-Allen and Schultz reported average myoelectric onset latencies following perturbed stance in this sequence: Ankle, knee, torso, shoulder [38]. Similarly, our findings suggest that responses to slip events are seen first in the legs and later in the arms. This may also support Tang and Woollacott's observations of distal-to-proximal reaction sequences from ankle to trunk [41].

6.3 HEAD ACCELERATION

A weak but statistically significant positive correlation between vertical head acceleration onset and left shoulder summed moment onset was found, when controlling for outcome. A study of perturbed stance (rearward directed treadmill acceleration) in healthy and vestibular-impaired subjects offered evidence that vestibular inputs are not necessary to trigger corrective hip muscle contractions [39]. In contrast, it has been shown that information about head motion from the vestibular system and information from proprioceptive afferents arrive at the central nervous system at approximately the same time. Further, vestibular system input affects perturbation response magnitude in the legs and trunk [2]. Previously, a study indicated that subjects released from a height displayed activation of the gastrocnemius 74ms following release, and this reaction was attributed to the vestibular system, independent of any stretch reflex [20]. The human vestibular system can detect accelerations as small as 0.15m/s^2 in the superior/inferior direction [5], indicating there is potential to detect vertical drop caused by slip. This potential slip detection modality must be further investigated as our results were not conclusive.

6.4 EFFECT OF SHOULDER DYNAMICS ON WHOLE BODY COM MOTION

Generating strong left flexion moments was associated with lesser disturbances of the whole-body COM. This may be due in part to the contribution of raised arms to changing the body's mass moment of inertia, reducing the tendency of the body to rotate. Shoulder flexion/extension moment generation and COM dynamics are certainly coupled by the arms as a component of the whole body COM, but the arms are a small part of overall COM, comprising ~8% of body mass [13]. It has been demonstrated with inverse dynamic simulations that bilateral shoulder flexion during stance shifts the whole-body COM forward [33]. Whole-body postural response including bilateral shoulder flexion in particular has been shown to reduce posterior displacement of the whole body COM in the sagittal plane, compared with other postural strategies involving the arms to a lesser extent [38]. Most importantly, it has been shown that arm activity during slip-like events raises the whole-body COM and decreases the deviation of the COM trajectory in the direction of the slipping foot [29]. Our findings support these previous findings concerning the effect of arm movement in controlling the whole-body COM disturbance during slip.

7.0 LIMITATIONS

The findings of this study must be considered within the limits of assumptions made about human movement and our efforts to model them. We model the body as a linkage of 15 rigid segments with idealized joints. In particular, the shoulder is a joint of great complexity, comprised of many bones, muscles, ligaments, and tendons. This study treats the shoulder as a spherical joint between the torso and the upper arm, which is a simplification. Shoulder moments were calculated with respect to the Cartesian reference frame of the torso, but calculation of shoulder angles employed a Joint Coordinate System approach. Thus, flexion/extension and ab/adduction kinematics and kinetics do not strictly correspond. The inverted-pendulum model of Aim 3 considers the body between the heel and the COM a single link, though it actually includes the knee and hip joints. At heel strike, the knee and hip are nearly fully extended. However, knee and hip responses are part of reaction to severe slips, which is not accounted for by the inverted pendulum model.

Each trial was examined only through 50% stance, because after that point it was not clear whether subjects' body motion was affected as they moved off of the slippery force platform, or by interference from the harness. Future studies might explore how the slip fully develops, i.e. experiment with a longer continuous slippery surface.

Angle and moment parameters were calculated from manually-chosen events. Knee and hip moment onsets were chosen by a different researcher than the other onsets in this study. Although the researchers have attempted to use the same method, inconsistencies are possible as subjective judgment is sometimes necessary to select an onset point.

We infer that the walking patterns of subjects who contributed data for this study represent the gait of human beings in general. We do not know how our experimental setup affected the subjects: By outfitting subjects in shoes, a harness, and tight clothing and asking them to walk in a dimly-lit room, we may have altered their gait.

One focus of the study is differences between older and younger subjects in dry and slippery conditions. There is a limit to the age of subjects that we are permitted to recruit and test in this experiment because of the dangers posed by slippery surfaces, and our “older” group might not be old enough to reveal subtle differences between age groups.

Only one slip trial could be analyzed as the unexpected slip condition. In this study, the population size was 29. A larger subject population could help reveal subtle effects in unexpected slips.

8.0 CONCLUSION

Subjects responded to perturbations of greater severity with greater-magnitude motions and moments, but not earlier moment onsets. Older subjects displayed weaker and later responses to slips. Shoulder response occurred significantly later than leg joint response. Head motion was correlated with onset of shoulder moments, but not strongly. Smaller COM perturbations were associated with strong flexion moment responses, suggesting that strong flexion moments of the shoulder on the ipsilateral side help correct imbalance in gait.

The findings presented in this research imply that arm responses play a role in balance recovery and that a legs-to-arms response sequence appears to drive the reaction to a slip. The potential contribution of the vestibular system in triggering arm motion cannot be ruled out. Finally, age-related effects on arm responses may aggravate the risk of slips and falls in older adults.

APPENDIX A

CONCERNING METHODS

Equation 1. The transfer function of the elliptical filter used to smooth angular position data:

$$H(x) = \frac{2.1965e^{-4} x^8 - 9.0363e^{-4} x^7 + 1.9192e^{-3} x^6 - 2.717e^{-3} x^5 + 3.007e^{-3} x^4 - 2.717e^{-3} x^3 + 1.9192e^{-3} x^2 - 9.0363e^{-4} x + 2.1965e^{-4}}{x^8 - 6.7835 x^7 + 20.368 x^6 - 35.328 x^5 + 38.691 x^4 - 27.384 x^3 + 12.226 x^2 - 3.1471 x + 0.35749}$$

BIBLIOGRAPHY

- [1] Alexander, B. H., Rivara, F. P., and Wolf, M. E., The cost and frequency of hospitalization for fall-related injuries in older adults *Am J Public Health*, vol. 82, pp. 1020-3, Jul, 1992.
- [2] Allum, J. H., Carpenter, M. G., and Honegger, F., Directional aspects of balance corrections in man *IEEE Eng Med Biol Mag*, vol. 22, pp. 37-47, Mar, 2003-Apr 30, 2003.
- [3] Allum, J. H., Carpenter, M. G., Honegger, F., Adkin, A. L., and Bloem, B. R., Age-dependent variations in the directional sensitivity of balance corrections and compensatory arm movements in man *J Physiol*, vol. 542, pp. 643-63, Jul 15, 2002.
- [4] Ballesteros, M.L., Buchtal, F., and Rosenfalck, P., The pattern of muscular activity during arm swing of natural walking *Acta Physiol Scand*, vol. 63, pp. 296-310, Mar, 1965.
- [5] Benson, A. J., Spencer, M. B., and Stott, J. R., Thresholds for the detection of the direction of whole-body, linear movement in the horizontal plane *Aviat Space Environ Med*, vol. 57, pp. 1088-96, Nov, 1986.
- [6] Berg, W. P., Alessio, H. M., Mills, E. M., and Tong, C., Circumstances and consequences of falls in independent community-dwelling older adults *Age Ageing*, vol. 26, pp. 261-8, Jul, 1997.
- [7] Beschorner, K., Margerum S , and Cham R, Center of mass dynamics during unexpected slips in young and older adults *Submitted to Journal of Biomechanics*, vol.
- [8] Bureau of Labor Statistics. Census of Fatal Occupational Injuries Summary, 2004. 2005.
- [9] Bureau of Labor Statistics. Employed persons in agriculture and related and in nonagricultural industries by age, sex, and class of worker. 2006.
- [10] Cejka, C., Lee, T. A., McIlroy, W. E., and Maki, B. E., Control of reach-to-grasp reactions during perturbed locomotion in familiar and unfamiliar environments: when does visual fixation of the handrail occur? *Proceedings of the XXth ISB Congress - ASB 29th Annual Meeting*, vol. Jul 31, 2005.(Abstract)

- [11] Chaffin, D. B. and Andersson, G. B. J. *Occupational biomechanics*, New York : Wiley, 1991.
- [12] Courtney, T. K., Sorock, G. S., Manning, D. P., Collins, J. W., and Holbein-Jenny, M. A., Occupational slip, trip, and fall-related injuries--can the contribution of slipperiness be isolated? *Ergonomics*, vol. 44, pp. 1118-37, Oct 20, 2001.
- [13] de Leva, P., Adjustments to Zatsiorsky-Seluyanov's segment inertia parameters *J Biomech*, vol. 29, pp. 1223-30, Sep, 1996.
- [14] DeGoede, K. M., Ashton-Miller, J. A., and Schultz, A. B., Fall-related upper body injuries in the older adult: a review of the biomechanical issues *J Biomech*, vol. 36, pp. 1043-53, Jul, 2003.
- [15] Dietz, V., Human neuronal control of automatic functional movements: interaction between central programs and afferent input *Physiol Rev*, vol. 72, pp. 33-69, Jan, 1992.
- [16] Dietz, V., Fouad, K., and Bastiaanse, C. M., Neuronal coordination of arm and leg movements during human locomotion *Eur J Neurosci*, vol. 14, pp. 1906-14, Dec, 2001.
- [17] Elftman, H., The function of the arms in walking *Human Biology*, vol. 11, pp. 529-535, 1939.(Abstract)
- [18] Fullerton, H. N., Labor force projections to 2008: steady growth and changing composition *Monthly Labor Review*, vol. 122, pp. 19-32, 1999.
- [19] Health and Safety Executive. Slips and Trips, 2005. 2006.
- [20] Jones, G. M. and Watt, D. G., Muscular control of landing from unexpected falls in man *J Physiol*, vol. 219, pp. 729-37, Dec, 1971.
- [21] Kirtley, C., Clinical gait analysis: theory and practice Anonymous2006. Elsevier Churchill-Livingstone. Philadelphia.
- [22] Maki, B. E. and McIlroy, W. E., The role of limb movements in maintaining upright stance: the "change-in-support" strategy *Phys Ther*, vol. 77, pp. 488-507, May, 1997.
- [23] Marigold, D. S., Bethune, A. J., and Patla, A. E., Role of the unperturbed limb and arms in the reactive recovery response to an unexpected slip during locomotion *J Neurophysiol*, vol. 89, pp. 1727-37, Apr, 2003.
- [24] McIlroy, W. E. and Maki, B. E., Early activation of arm muscles follows external perturbation of upright stance *Neurosci Lett*, vol. 184, pp. 177-80, Jan 30, 1995.

- [25] Misiaszek, J. E., Early activation of arm and leg muscles following pulls to the waist during walking *Exp Brain Res*, vol. 151, pp. 318-29, Aug, 2003.
- [26] Moyer, B. E., Chambers, A. J., Redfern, M. S., and Cham, R., Gait parameters as predictors of slip severity in younger and older adults *Ergonomics*, vol. 49, pp. 329-43, Mar 15, 2006.
- [27] Moyer, B., *Slip and fall risks: Pre-slip gait contributions and post-slip response effects* Pittsburgh: University of Pittsburgh, 2006.
- [28] Murray, M. P., Sepic, S. B., and Barnard, E. J., Patterns of sagittal rotation of the upper limbs in walking *Phys Ther*, vol. 47, pp. 272-84, Apr, 1967.
- [29] Oates, A. R., Patla, A. E., Frank, J. S., and Greig, M. A., Control of dynamic stability during gait termination on a slippery surface *J Neurophysiol*, vol. 93, pp. 64-70, Jan, 2005.
- [30] Palvanen, M., Kannus, P., Parkkari, J., Pitkajarvi, T., Pasanen, M., Vuori, I., and Jarvinen, M., The injury mechanisms of osteoporotic upper extremity fractures among older adults: a controlled study of 287 consecutive patients and their 108 controls *Osteoporos Int*, vol. 11, pp. 822-31, 2000.
- [31] Pavol, M. J. and Pai, Y. C., Feedforward adaptations are used to compensate for a potential loss of balance *Exp Brain Res*, vol. 145, pp. 528-38, Aug, 2002.
- [32] Personick, M. E. and Windau, J. A., Characteristics of older workers' injuries. 891, *U.S. Department of Labor - Bureau of Labor Statistics*, vol. 1995.
- [33] Pozzo, T., Ouamer, M., and Gentil, C., Simulating mechanical consequences of voluntary movement upon whole-body equilibrium: the arm-raising paradigm revisited *Biol Cybern*, vol. 85, pp. 39-49, Jul, 2001.
- [34] Quant, S., Maki, B. E., Verrier, M. C., and McIlroy, W. E., Passive and active lower-limb movements delay upper-limb balance reactions *Neuroreport*, vol. 12, pp. 2821-5, Sep 17, 2001.
- [35] Rice, D. P. and MacKenzie, E. J., Cost of injury in the United States : a report to Congress Anonymous 1989. Injury Prevention Center, School of Hygiene and Public Health, The Johns Hopkins University. Baltimore.
- [36] Rivara, F. P., Grossman, D. C., and Cummings, P., Injury prevention. Second of two parts *N Engl J Med*, vol. 337, pp. 613-8, Aug 28, 1997.
- [37] Roberts, T. *Neurophysiology of postural mechanisms* , Woburn, MA: Butterworth, 1978.
- [38] Romick-Allen, R. and Schultz, A. B., Biomechanics of reactions to impending falls *J Biomech*, vol. 21, pp. 591-600, 1988.

- [39] Runge, C. F., Shupert, C. L., Horak, F. B., and Zajac, F. E., Role of vestibular information in initiation of rapid postural responses *Exp Brain Res*, vol. 122, pp. 403-12, Oct, 1998.
- [40] Sattin, R. W., Falls among older persons: a public health perspective *Annu Rev Public Health*, vol. 13, pp. 489-508, 1992.
- [41] Tang, P. F. and Woollacott, M. H., Inefficient postural responses to unexpected slips during walking in older adults *J Gerontol A Biol Sci Med Sci*, vol. 53, pp. M471-80, Nov, 1998.
- [42] Tang, P. F. and Woollacott, M. H., Phase-dependent modulation of proximal and distal postural responses to slips in young and older adults *J Gerontol A Biol Sci Med Sci*, vol. 54, pp. M89-102, Feb, 1999.
- [43] Tinetti, M. E., Speechley, M., and Ginter, S. F., Risk factors for falls among elderly persons living in the community *N Engl J Med*, vol. 319, pp. 1701-7, Dec 29, 1988.
- [44] Winter, D. A., *Biomechanics and Motor Control of Human Gait: Normal, Elderly and Pathological*, 2nd ed. Waterloo: Waterloo Biomechanics, 1991.
- [45] V.M. Zatsiorsky. *Kinematics of human motion*, Champaign, IL: Human Kinetics, 1998.